X-ray Diffraction Analysis of Mudstone from NW Sudan

BY
SUAD Z.ELABDEEN SALIH

A Thesis Submitted for the partial fulfilment of the requirements of degree of master of Science

Department of Physics
Faculty of Science
University of Khartoum

March 1997

We regret that some of the pages in this report may not be up to the proper legibility standards, even though the best possible copy was used for scanning

CONTENTS

ACKNOWLEDGEMENTS

I am greatly indebted to my former supervisor Dr. Osman Dawi Eisa who introduced the method of this work. Dr. Eisa's help and continuous follow-up are highly appreciated.

All thanks are due to Dr. O. M. Abdullatif, Department of Geology, who continued the supervision of this work, for his assistance and guidance.

My thanks also to Dr. A/Rahman Osman and A/ aydabi for their help in typing and printing this work.

At last and not least my all thank to Mr. Hassan Hag Elhussain for his invaluable help.

ABSTRACT

This study deals with the theoretical and experimental aspects of the X-ray diffraction technique (XRD). The XRD Technique is used to investigate fine structure of matter, and it is most efficient method for the determination of the mineralogical composition of rocks.

The XRD technique is used also to investigate the clay mineralogical composition of mud-stones of the Nubian sandstone of north western Sudan.

The XRD results revealed that the mud–stone samples are composed, in decreasing abundance's of kaolinite, smectite, chlorite and illite. Non-clay minerals reported include quartz, feldspars and geothite. Kaolinite dominates in most of samples with percentages ranging between 78 – 96% Smectite comes second in abundance and ranges between 10 – 24%,followed by chlorite and illite which show the lowest abundance's.

The dominance of kaolinite over smectite indicates that intense chemical weathering and leaching occurred under warm humid climate interrupted by dry periods. Most probably these clay minerals were produced by inheritance and partly by neoformation. The variation of the chemical composition of these mud stones is due basically to differences in clay mineralogy which was controlled by source rock geology, weathering physiochemical behavior of elements, local environment and climatic condition in the past.

CHAPTER I

INTRODUCTION

1-0 Introduction

X-ray diffraction (XRD) is used to investigate fine structures of matter. It began in Van laue's discovery in (1912) when he showed that, if the atoms in crystal were arranged in regular way, a crystal might serve as a three dimensional grating to diffract a beam of the newly discovered Roentgen X-rays (1895).

In most X-ray diffraction experiments the X-ray beam has a diameter of the order of 1 mm. For certain applications, for example in cases where it is necessary to examine a very small area of the specimen, beams of much smaller *diameter are required.* (Pieser et al, 1955).

One of the most efficient method for the determination of the mineralogical composition or rocks is the X-ray diffraction. The complex structures of these minerals can be revealed by this method.

These include clay minerals which occur mostly in sedimentary rocks, such as sandstones, mudstones, claystones and limestones (Tucker, 1991).

To determine the petrology of rocks sediments, depositional environments, provenance studies of burial history, the knowledge of the clay mineralogy can be used.
Moreover, the determination of clay minerals has an important industrial application in engineering, chemical and ceramics industries.(Grim, 1962).

A knowledge of mineralogy is highly important for geological prospecting exploration and evaluation of the economics potential of mineral deposits. This depends on accurate identification of the minerals, knowledge of the composition and association in which they occur in nature.

Minerals are natural chemical compounds and are natural product of various physio-chemical processes going on the earth crust, including the products of the life activity of various organisms.

(I-1) Clay Minerals:-

Clay minerals are most abundant minerals on the surface of the earth. This is illustrated by the fact that they are the essential constituents of fine sedimentary rocks, such as mud stones, clay-stones and shells making up to 75% of the total sediments composition. They are hydrous alumino silicate with specific sheet or layered structures.

The typical size of clay minerals is less than 2μ but they may reach 10μ or more. Common clay minerals include kaolinite, illite , smectite and chlorite.

(I-2) Formation and Distribution of Clay Mineral

Clay minerals in sedimentary rocks have three origins:-

(a) Inheritance.
(b) Neoformation.
(c) Transformation.

These processes occur in the weathering and soil environment, depositional environment and during diagencsis (Tucker 1991).

In the first, the clay are detrital and have been formed in another area, and they are stable in their present location. In the second, the clays have formed in situ, and they have either been precipitated from solution or formed from amorphous silicate material.

In the third, the clays will carry a memory of inherited characteristic from the source area with chemical environment. (Weaver, 1989 and Curtis, 1990).

These processes resulting from the interaction between the rocks, the air, the water and the organisms are referred to as weathering (Chamley ,1989).

The clay-minerals formation take place in three major locations:-

1. In the weathering and soil environment.
2. In the depsitional environment.
3. During diagencsis and into low grade metamorphism (Tucker, 1991).

1-3 Objective and scope of work:

This work deals with the theoretical and experimental aspect of XRD. Moreover, XRD technique is used to determine the mineralogical composition of sedimentary rocks samples collected from different areas in North West Sudan (fig I-1).

The aim of this work is :

1.To determine the clay mineralogy of some mud stone samples from that area.

2 To know the origin of these clay minerals and their depositional environment.

XRF was used to supplement the (XRD) studies of rocks and to characterize their chemical elements composition. Also the concentration of these elements were determined.

The format of thesis will be as follows:-

The elementary theory of crystallographic notation and XRD theory will be discussed in chapter II (Theoretical Background). In chapter III the experimental set-up, data processing with DACO-MP, sample preparation and data collection are given. A note on the DIFFRAC-AT software is also given.

Chapter IV deals with the data analysis and results obtained, and finally the conclusions and suggestions are given in chapter V.

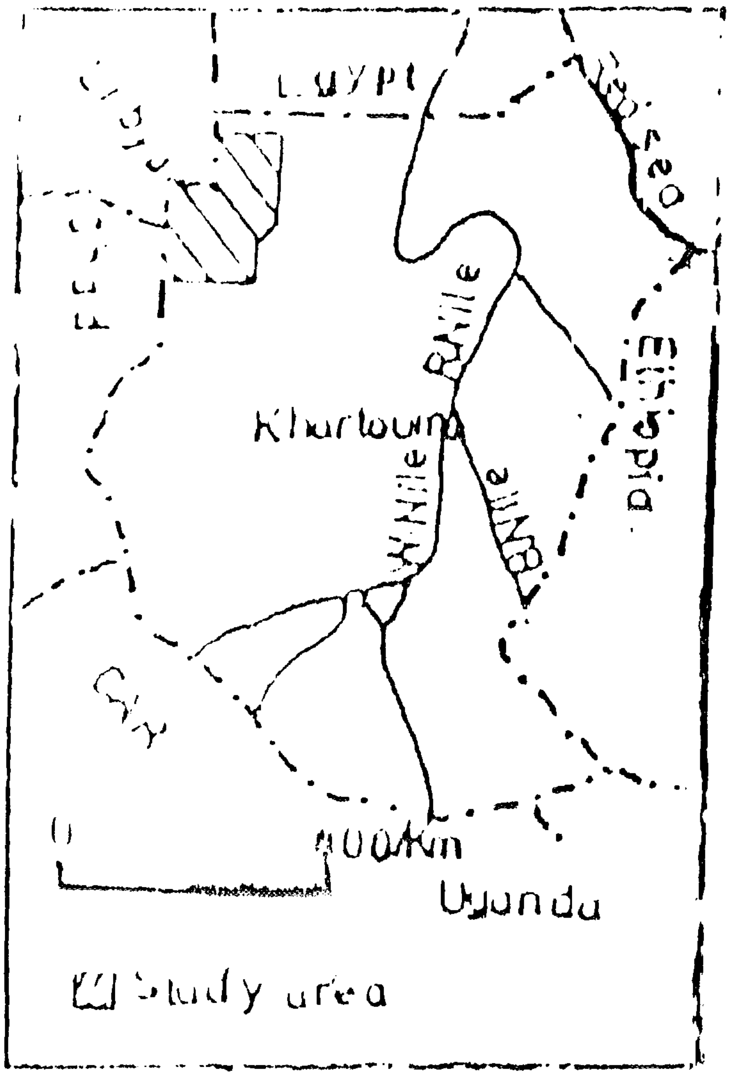
Egypt
Khartoum
R.Nile
W.Nile
B.Nile
Ethiopia
CAR
0
400Km
Uganda
Study area

CHAPTER II

THEORETICAL BACKGROUND

0) Introduction:-

In this chapter the theoretical aspects of crystal notation and XRD are briefly reviewed, namely; the crystal, the crystal lattice miller indices, the unit cell , the reciprocal lattice, Bragg law of diffraction and intensity of diffraction as well as the factors affecting it.

- 1) The Crystalline Solid :-

A crystal is defined as a three dimensional structural pattern obtained through repetition of a specified unit pattern or unit cell periodically throughout the body of the material (Nuffield, 1960).

I - 2) The Crystal Lattice :-

An ideal crystal is the one without structural defects, such as vacancies, impurities or grain boundaries.

The distribution of atoms in such a crystal may be represented by a lattice of points in space, defined by infinite set of lattice vectors given by (Cullity, 1978):

$$L = L_1 a_1 + L_2 a_2 + L_3 a_3 \qquad \textbf{(II - 1)}$$

where L_1, L_2, L_3 are integers.

If there is only one species of atoms on the lattice sites, the lattice is called a Bravais Lattice (Fig. II-l-a). If there is group of atoms in the crystal, the lattice site may be associated not with one atom but with a set of atoms, hence the lattice has a basis and is called a lattice with a basis (Fig. II-l-b) (Alexander and Animalu, 1981).

II - 3) The Unit Cell :-

The scheme of repetition is defined by three vectors a_1, a_2, a_3 called the crystal axes. It is only the magnitude and direction of the repeating isplacements are of importance. The position chosen as origin is immaterial. he parallelepiped make up the crystal. The smallest volume is called the unit ell. The unit cell volume is given by :

$$Va = a_1 \cdot a_2 \times a_3 \qquad \text{(II - 2)}$$

- 4) The Crystallographic Notations :-

The Miller indices for a plane are sets of integers, *h, k, l,* for a cabin *1/h, 1/k, 1/l* are the intercepts of the plane *(hkl)* on the a_1, a_2, a_3 axes, so that the equation of the plane may be written as :

$$\frac{X}{1/h} + \frac{Y}{1/k} + \frac{Z}{1/L} = 1 \qquad \text{(II - 3)}$$

$$hX + kY + lZ = 1 \qquad \text{(II - 4)}$$

. (II-2) shows a plane specified by the Miller indices *(hkl)*

- 5-a) The Reciprocal Lattice :-

The vectors H_{hkl} are drawn for all values of the indices *hkl*. The terminal points of these vectors form a new lattice with repetition vectors b_1, b_2, b_3.

This lattice is called the reciprocal lattice.

- 5-b) The Reciprocal Vectors :-

The crystal axes a_1, a_2, a_3 can be used to define the reciprocal vectors b_1, b_2, b_3.

$$b_1 = \frac{a_1 \times a_3}{a_1 \cdot a_2 \times a_3} \qquad \text{(II-5)}$$

$$b_2 = \frac{a_1 \times a_3}{a_1 \cdot a_2 \times a_3} \qquad \text{(II-6)}$$

$$b_3 = \frac{a_1 \times a_2}{a_1 \cdot a_2 \times a_3} \qquad \text{(II-7)}$$

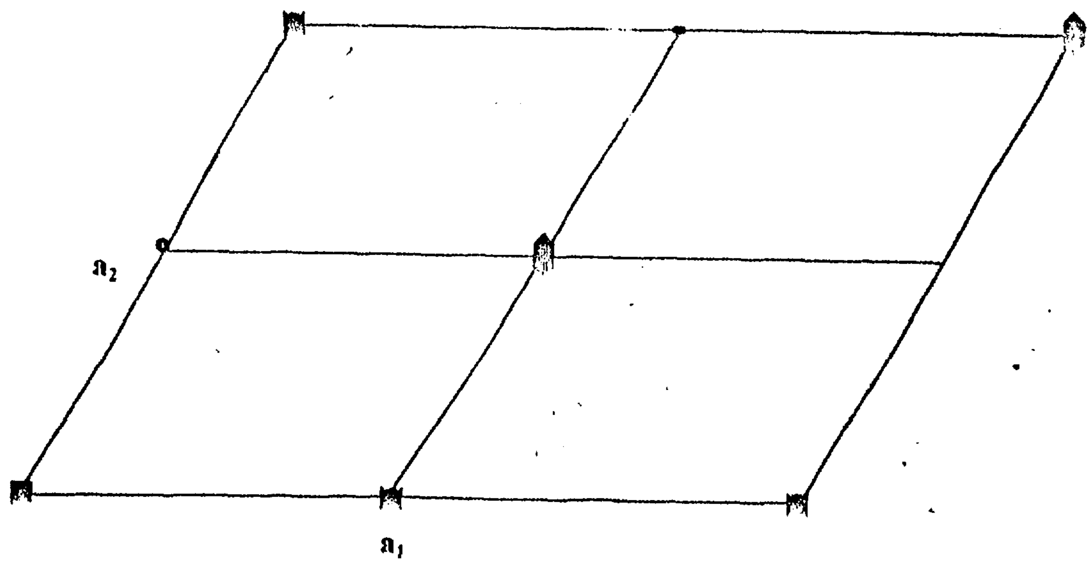

Fig. (II-1-a) Two dimensional lattice
Bravais Lattice

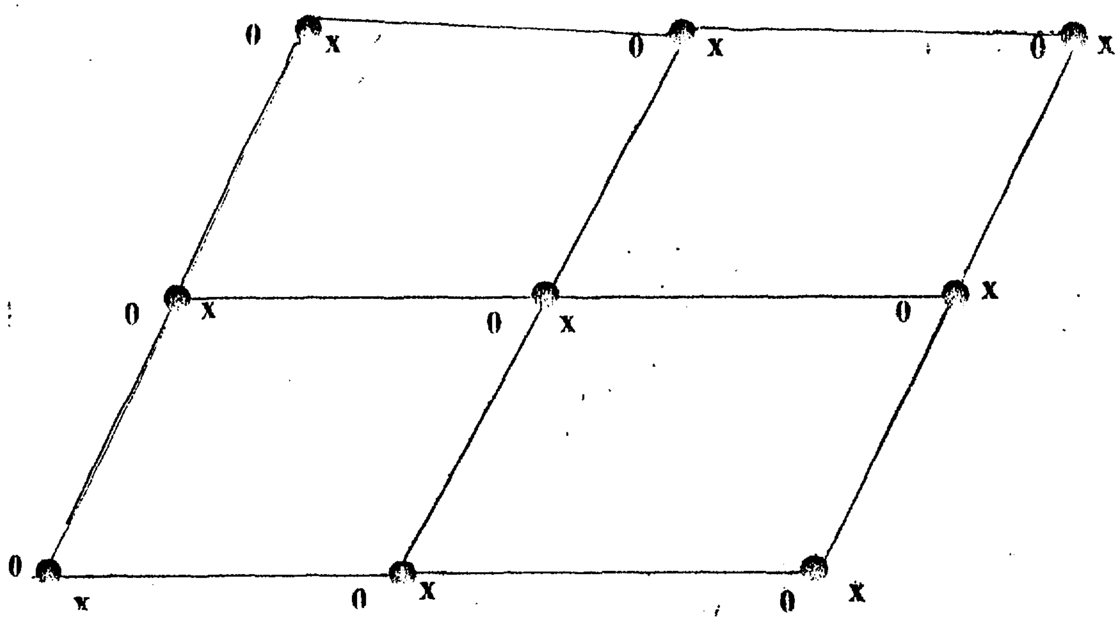

Fig. (II-1-b) Lattice with a basis of three atoms •, O, X

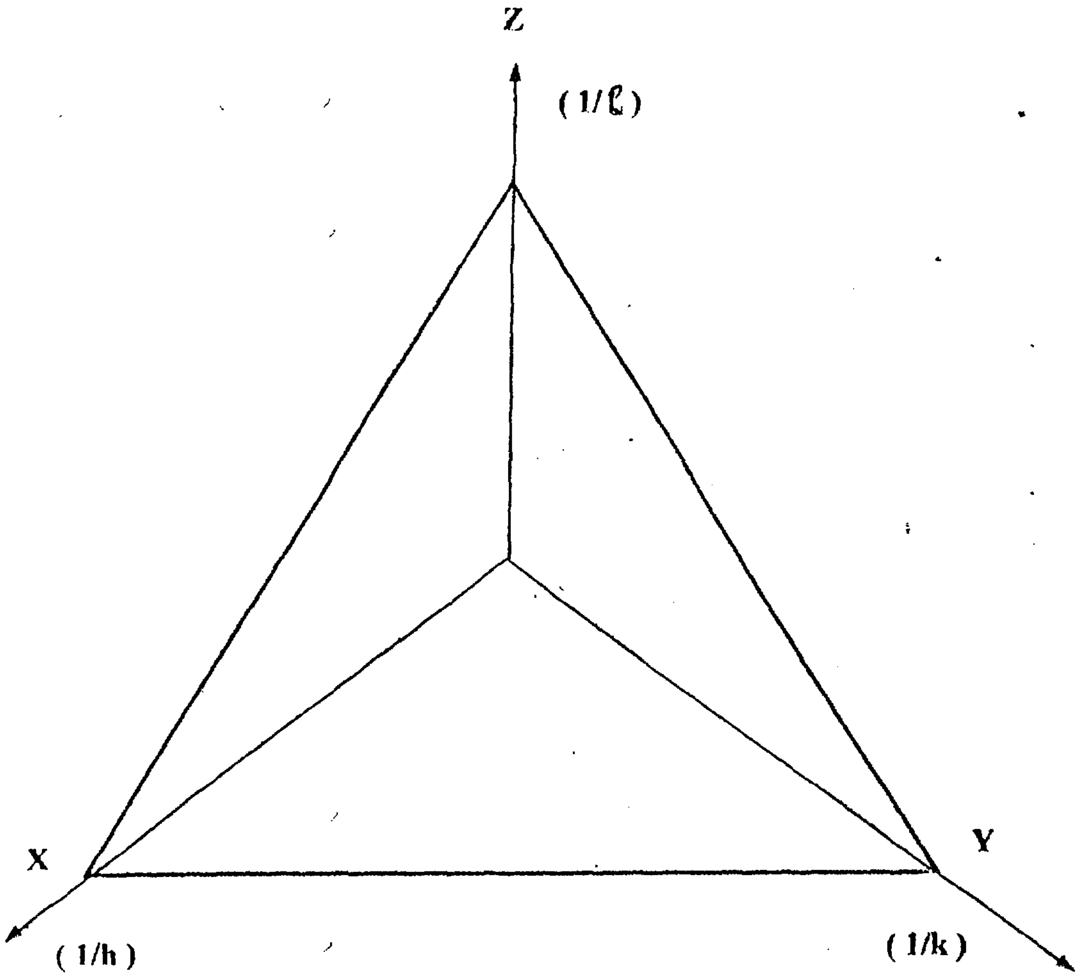

Fig.(II-2) A plane specified by the Miller indices (*hkl*)

Each reciprocal vector is perpendicular to the plane defined by two crystal axes having different indices.

An important relation between the two sets of vectors is expressed by the scalar products.

If the indices are the same :

$$a_1 \cdot b_1 = a_1 \cdot \frac{a_2 \times a_3}{a_1 \cdot a_2 \times a_3} = 1 \qquad \text{(II - 8)}$$

If the indices are different :

$$a_1 \cdot b_2 = a_1 \cdot \frac{a_1 \times a_3}{a_1 \cdot a_2 \times a_3} = 0 \qquad \text{(II - 9)}$$

The vector H_{hkl} is defined in terms of the reciprocal vectors and the Miller indices :

$$H_{hkL} = hb_1 + kb_2 + Lb_3 \qquad \text{(II - 10)}$$

(II - 6) X-ray Diffraction :-

The phenomenon of X-ray diffraction by crystals has proved to be an invaluable tool of the physicist, both as a method of measuring X-ray wave-length and of studying the structure of crystal.

X-rays from part of the electromagnetic radiation spectrum and of the energy E of an X-ray photon is related to the wave-length by Planck's hypothesis.

$$E = hc / \lambda \qquad \text{(II - 11)}$$

The simplest explanation of the observed diffraction pattern which result from the passage of X-rays through a crystal was first derived by Bragg in 1913.

Bragg considered an X-ray wave front incident on a surface row of atoms in the crystal will combine as they fall on top of one another in a random manner fig (II-3).

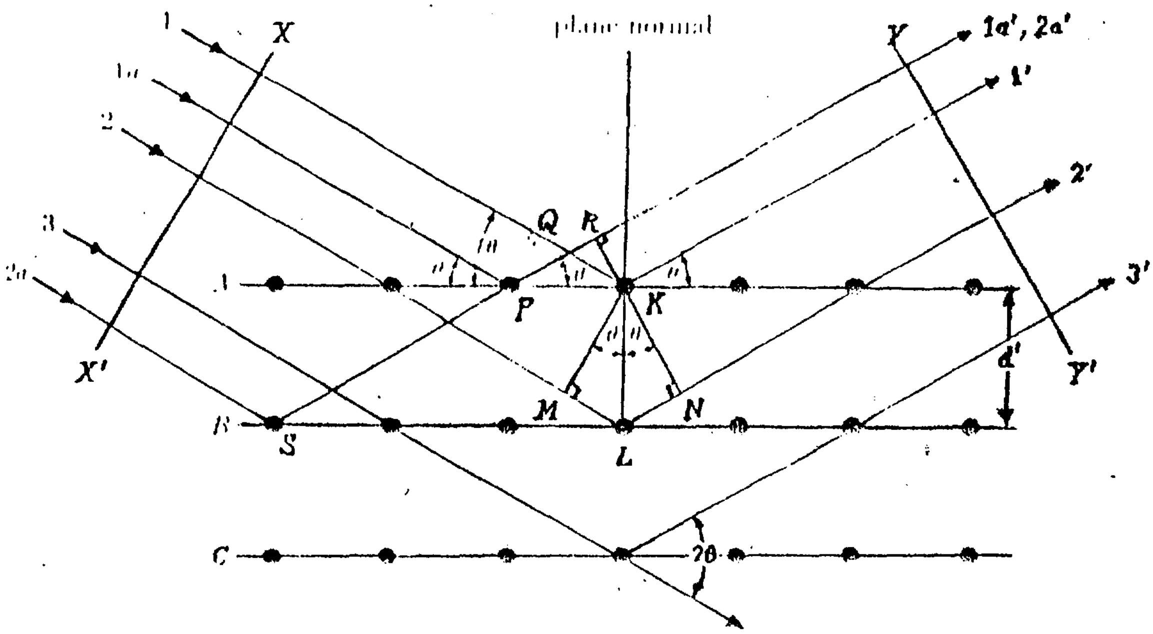

Fig.(II-3) Diffraction of X-rays by a Crystal

In perfect crystal where the X-rays scatter without loss of energy, the incident waves are reflected specularly from parallel planes of atoms and constructive interference may occur.

Rays from a series of crystal planes spaced equal distance "d" apart fall on top of each other. It is well known from the principle of interference of waves, constructive interference occurs whenever the path difference from rays reflected from adjacent planes is :

$$2d\sin\theta = n\lambda \qquad \text{(II - 12)}$$

where n = 1, 2, 3

This is known as Bragg's Law (Cullity, 1987).

The planes of atoms in the crystal that are responsible for Bragg reflection are called Bragg planes.

The series of planes corresponding to :

$$n = 1, 2, 3, \ldots\ldots$$

correspond to first, second, third, ... order Bragg reflections. θ is the glancing angle or half the angle between the incident and reflected beams.

(II - 7) The Bragg Law :-

Two geometrical factors :-

1. The incident beam, the normal to the reflecting plane, and the diffracted beam are always coplanar.

2. The angle between the diffracted beam and incident beam is always 2θ, which is known as the diffraction angle.

Diffraction in general occurs only when the wave-length of the wave motion is of the same order of magnitude as the repeat distance between scattering centres. Since "$\sin\theta$" can not exceed unity, we may write :

$$\frac{n\lambda}{2d} = \sin\theta < 1 \qquad \text{(II - 13)}$$

If the coefficient of λ is now unity, then we write the Bragg Law in the form :

$$\lambda = 2d\sin\theta \qquad \text{(II - 14)}$$

An order reflection from (*hkl*) planes of d spacing may be considered as the first-order reflection from (n_h, n_k, n_l) planes of spacing :

$$d = d'/n$$

$$d(001) = \frac{\lambda}{2}\sin\theta(001) \qquad \text{(II-15)}$$

(II - 8) The Intensity of Diffraction :-

(II - 8-1) Scattering by an electron :-

X-rays are scattered in all directions by an electron, the intensity of the scattered beam depends on the angle of scattering.
The intensity I of the beam scattered by a single electron of charge 'e' rest mass 'm' at a distance 'r' from the electron is given by :

$$I_e = I_o\left(\frac{\mu}{4\Pi}\right)^2 \left(e^4 / m^2 r^2\right)\sin^2 \propto \qquad \text{(II - 16)}$$

I_e	=	Intensity at distance R from free electron.
I_o	=	Intensity of the incident beam.
μ_o	=	$4\Pi\times10^{-7}\,mkgC^{-2}$.
α	=	The angle between the scattering direction and the direction of the acceleration of the electron.

Fig. (II-5) represents an electron at O that scatters an incident beam along a direction OP with angle 2θ .This beam may be resolved into two plane-polarized components, having electric vectors E_y and E_z. The intensity at P is obtained by summing the intensities of these two scattered components.

$$Ip = Ip_X + Ipz$$

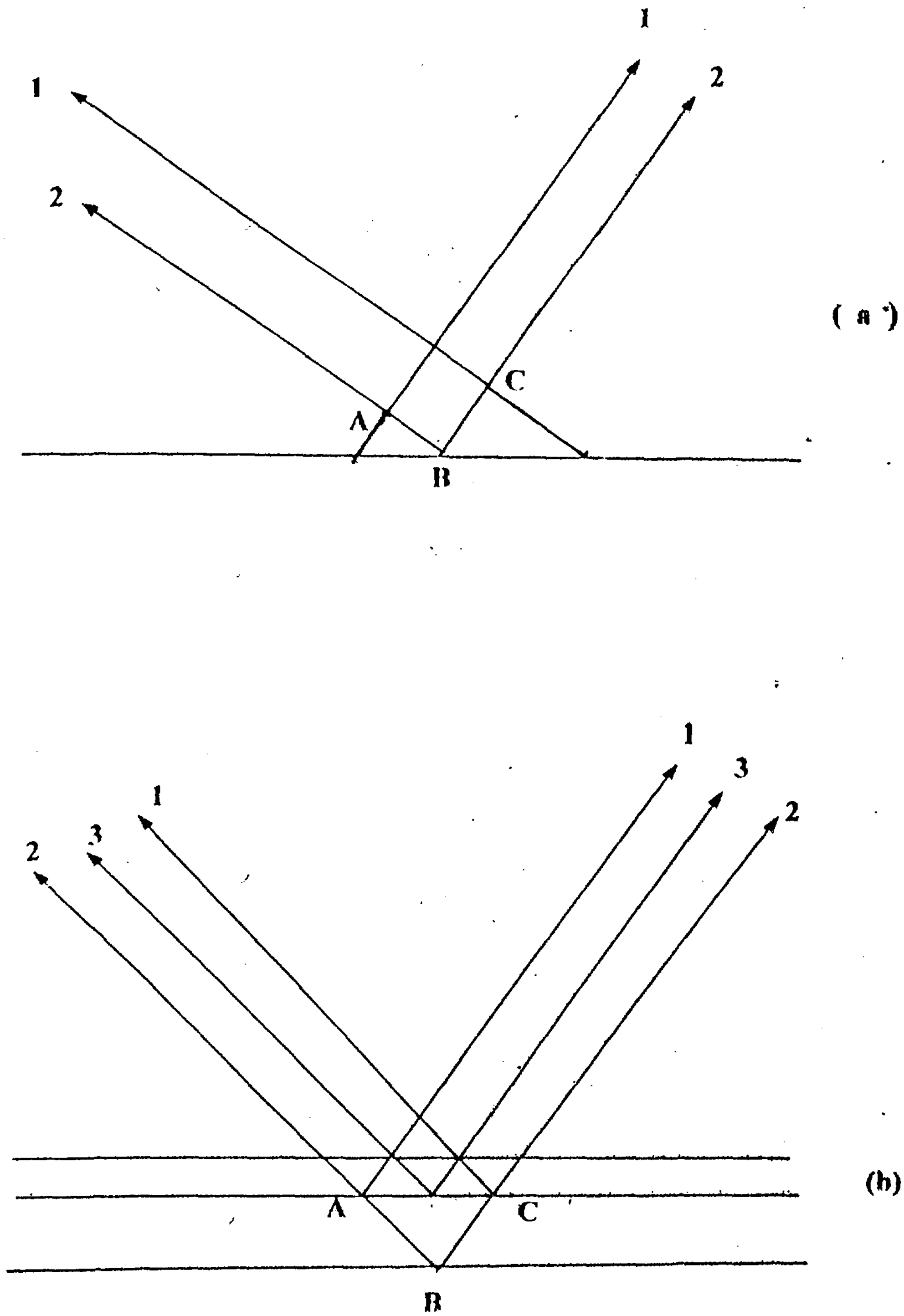

Fig. (II-4) (a) and (b)
Equivalence of (a) a second -order (100) reflection and a first-order (200) reflection

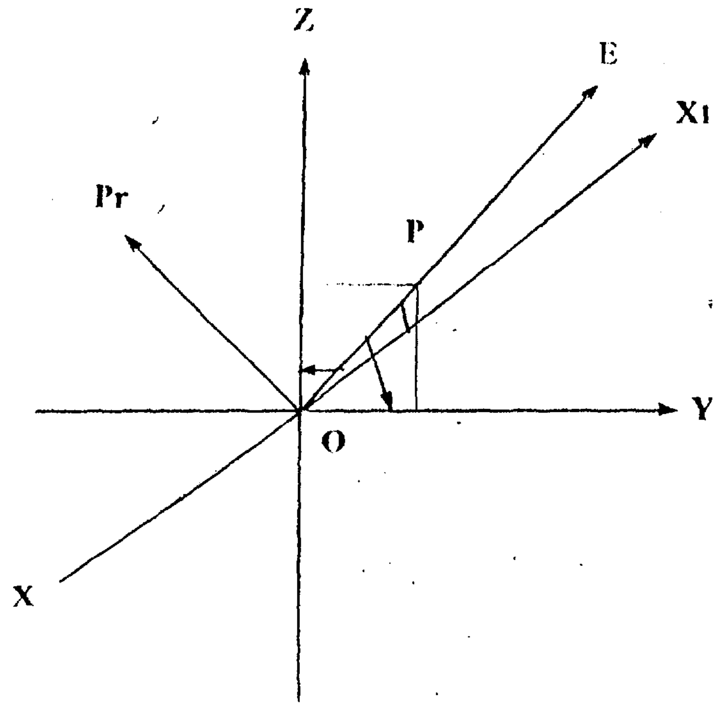

Fig. (II-5) Polarization of radiation scattered by an electron

$$Ip_X = I_{OY}\frac{k}{r^2}, Ip_Z = I_{OZ}\frac{k}{r^2}COS^2 2\theta$$

where

$$K = \frac{e^4}{m^2c^4}$$

or

$$Ip = \frac{k}{r^2}\left(I_{OY} + I_{OZ}COS^2 2\theta\right)$$

$$= \frac{k}{r^2}\left(\frac{I_O}{2} + \frac{I_O}{2}COS^2 2\theta\right)$$

$$= I_O\frac{K}{r^2}\left(\frac{1 + COS^2 2\theta}{2}\right) \qquad \text{(II-17)}$$

The factor $\frac{1}{2}\left(1 + COS^2 2\theta\right)$ is called the polarization factor.

(II - 8-2) Scattering by an atom :-

The efficiency of scattering of a given atom in a given direction is known as atomic scattering factor 'f' which is defined as a ratio of amplitude :

$$f = A_A / A_e \qquad \text{(II-18)}$$

Where A_A = The amplitude of the wave scattered by an atom .

A_e = The amplitude of the wave scattered by an electron.

The intensity of wave is proportional to the square of its amplitude :

$$I_A \propto f^2$$

$$I_A = I_e.f^2 \qquad \text{(II - 19)}$$

Where I_A and I_e are the intensities of the beam from the whole atom and the electron respectively.

NEXT PAGE(S) left BLANK

Chapter III

EXPERIMENTAL TECHNIQUE AND DATA PROCESSING

(III - 0) Introduction:

The role of this chapter is to describe the experimental set up and the techniques used for the analysis of the measurement.

The experimental method of X-ray generation with its accompanying cooling system and the monochromtaization are described below.

The system setup, the sample preparation of clays, the data collection and the methods of data analysis with both DACO-MD ANALYSES program and DIFFRAC -AT software are also given.

(III - 1) The Production of X-Rays :-

X-rays are produced whenever targets of heavy metals are bombarded by fast electrons. They exhibit arrow spikes at wave lengths characteristic of the target material (Fig. III - 1).

An X-ray tube is usually made up of :-

(1) A source of electrons.
(2) A high accelerating voltage.
(3) A metal target.

Most of the electrons that strike the target undergo numerous glancing collisions, with their energy going simply into heat.

A few electrons, though, lose most or all of their energy in single collisions with target atoms, with this energy evolved as X-rays.

(III - 2) The X-ray Generator :-

The generator used in this study is Siemens k710h and [k710] which is highly powered [2700 w]. It can be used for both X-ray diffraction and spectrometry applications Fig. (III - 2).

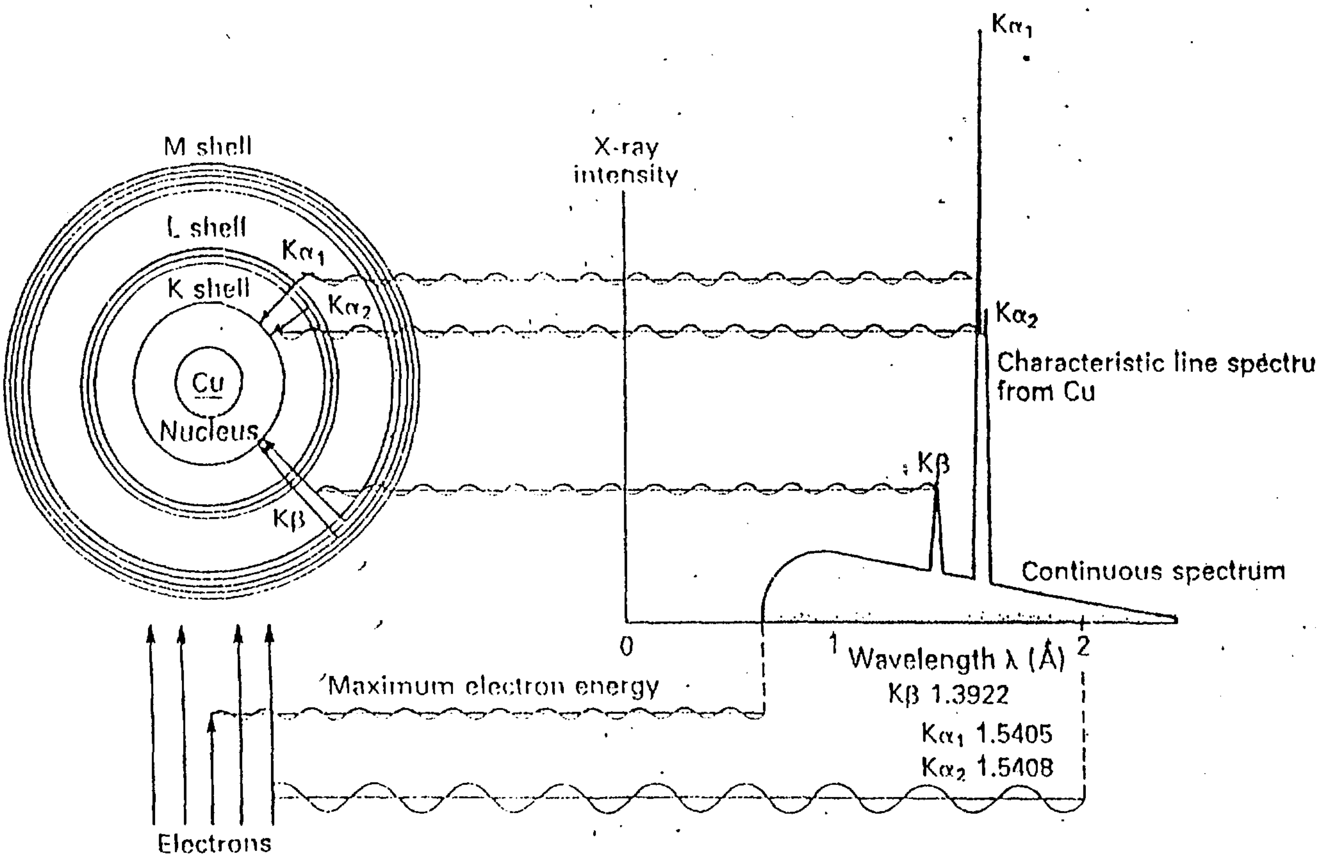

Fig. (III-1) X-Ray Generator

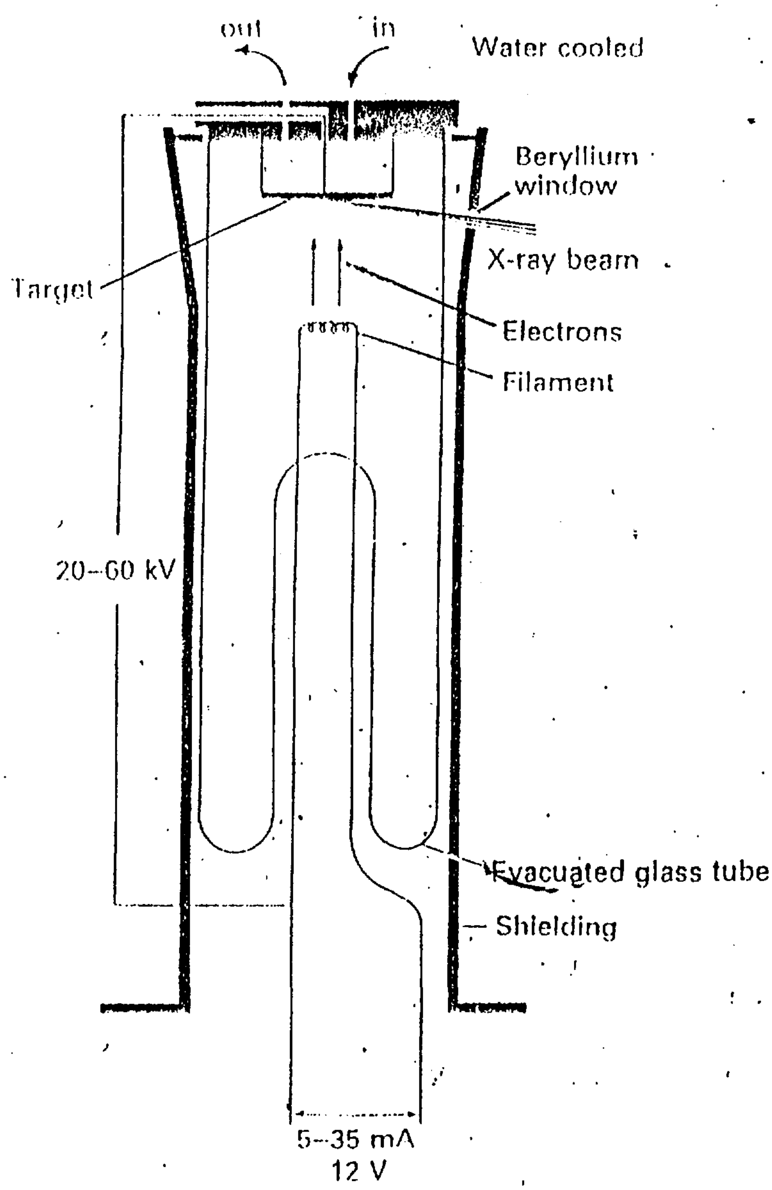

Fig. (III-2) A section of Rontgen X-ray tube

The generator supplies the X-ray tube with negative polarity high voltage form 20 kv to 55 kv **and current** of 5 mA to 60 mA .

(III - 3) The Diffractometer :-

The diffractometer used in this study is D500 Seimens. The radiation emanating from the line focus B of the x-ray tube is diffracted at the specimen PO1 and recorded by the detector D. (Fig. III - 3).

The specimen is rotated at constant angular speed , where as the detector moves about the specimen at double the angular speed .

The diffraction angle (2θ) is thus always equal to double the glancing(θ).

The beam path of the diffractometer is shown in fig (III - 3). Whenever the Bragg condition is fulfilled , the primary beam is reflected at the specimen to the detector. The intensity of the reflected radiation is measured by means of the detector connected to the electric measuring system , while the angle position of the reflections is indicated at the goniometer.

The focus, the specimen, and the detector. Diaphragm are located on the focusing circle F, the focus and the detector diaphragm are also located on measuring circle M.

The entire effective surface of the specimen would have to be located before the reflection reaches the detector

(III - 4) The Cooling System :-

The cooling unit, which is WKUVLER unit, is delivered with all components of the cooling circuit such as circulating pump, vaporising cooler, temperature controller, temperature monitor, antifreeze protection screwed connection, flow monitor, storage tank, safety value for max pressure limiting and connecting leads readily installed . .

The heated out let water enters the storage tank vice flow monitor and vaporizer. This tank is connected to the atmosphere.

The circulating pump aspirates this water from the tank and pumps it into the inlet connection .

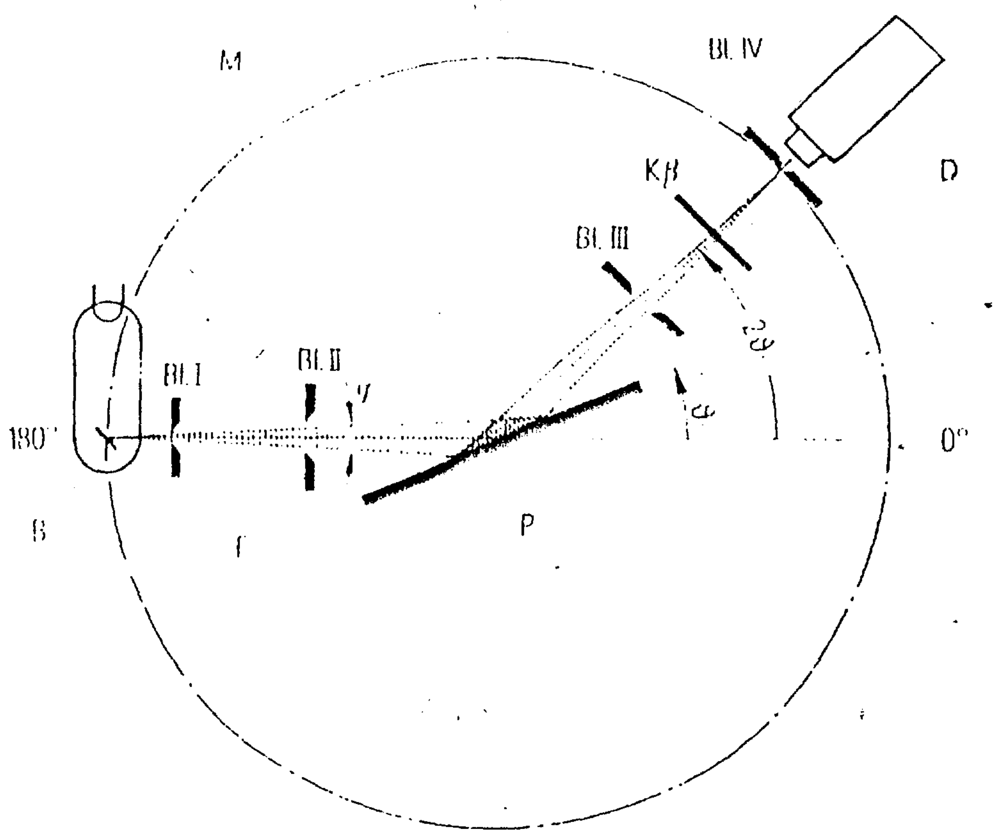

B'	Focus of the x-ray tube	ϑ	Glancing angle
Bl.I,II,III	Aperture diaphragms	2ϑ	Diffraction angle
Bl.IV	Detector diaphragm	φ	Aperture angle
D	Detector	M	Measuring circle
Kβ	Kβ filter	F	Focusing circle
P	Specimen		

Fig. (III-3) Focusing Geometry of the diffractometer in case of 2θ/θ

At an adjustable maximum pressure, the circulating medium is returned internally via an overflow valve .

The safety circuit monitors the cooling water supply to the consuming unit. It consists of a flow monitor which opens the circuit at an adjustable minimum circulating quantity, and a thermostat which also opens the circuit when an adjustable max-cooling water temperature is exceeded. Both devices are reset automatically. (Fig. III - 4).

(III - 5) The Goniometer :-

The diffractometer consists of a goniometer and the attachments required for the measurement. It is mounted either upright or horizontally in the radiation housing or on a separate table .

The specimen can be changed and observed inside the diffractometer super structures through a leadglass window at the front of the radiation protection. The diffractometer can be used in all applications of X-ray diffraction techniques, such as structure determination and phase analysis .

(III - 6) Monchromotization :-

Monochromatic beam of X-rays is desirable for certain diffraction studies, specially when the sample is a powder one . The reason for this is that the $K_\beta$component of the beam is sufficiently intense to produce its own diffraction pattern.

When this is superimposed on the K_α pattern, the difficulty of interpreting the diffraction effects is materially increased.

The absorption effect offers means of removing the unwanted radiation to leave a beam that is essentially monochromatic . The Nickel element (Ni) has an absorption edge of 1.49A^o, which is intermediate between the wave length of Cu K_β (1.5412A^o) and Cu K_α (1.3922A^o) radiation .

This element is, therefore, relatively transparent to the -radiation and absorbs the B component of X-ray beam and it can also reduce the intensity of the continuous spectrum.

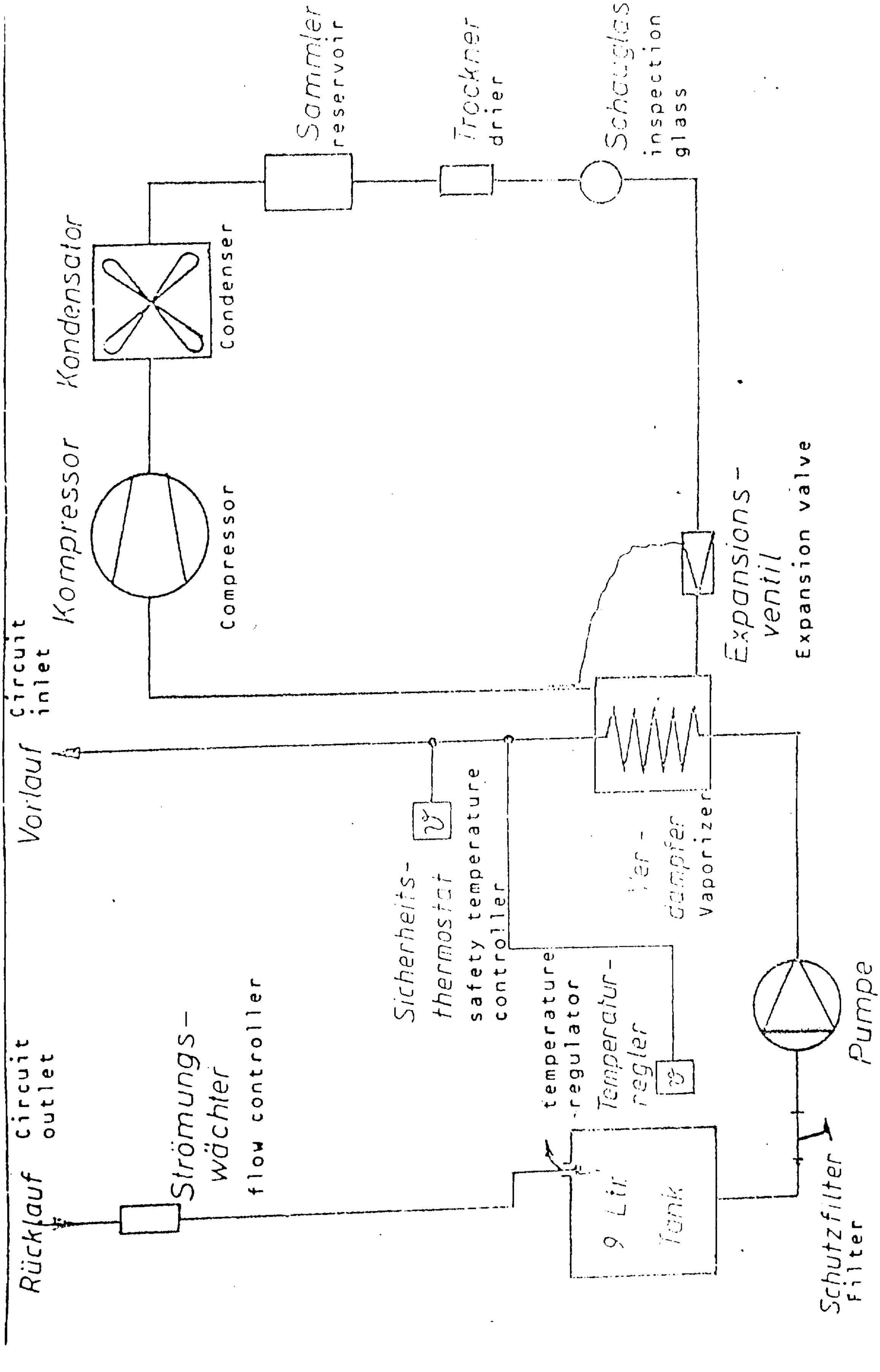

Fig.(III-4) The cooling system

(III - 7) The Detector :-

The detector normally used is a type NIM scintillation counter which can be used to measure X-radiation in the wave length range from 0-05 nm to 0-27 nm.

The radiation inlet window of the detector is made of thin beryllium or thin foil and must not be touched .

(III - 8) The DACO-MP:-

The DACO-MP is a micro computer with standard controller interfaced to the Siemens D500 diffractometer. It has 32 k bytes of ROM and 32 K bytes of RAM and normally controls a one or two circles diffractometer with one detector. When used as stand-alone (Diffractometer and the printer) controller for D500 or other diffractometers, the DACO-MP may control any measurement and also perform complex computations.

It is companion unit is an alphanumeric tele-printer allowing dialogue and graphic output diffractograms .

The DACO-MP software is logically made up of seven tasks that may potentially run in parallel :-

(I) The sequence for analytical programs stored in memory.
(II) The completion of time consuming commands.
(III) The initialization routines for commands from the computer .
(IV) The computer input processor task .
(V) The error message output task .
(VI) The display up date task .
(VII) The local terminal input and command initialization task .

All these tasks depend on or are controlled by the type of command used for performing a certain job.

Each command is associated with two fixed flag sets, one for the bare command and another for the command of one more explicit argument.

The user RAM is divided into four buffers, instruction buffer (I-buffer), data buffer (D-buffer), Registers buffer (Regs) and the secondary memory area (matrix) .

The DACO-MP provides writing and executing programs using its acceptable commands for many treatments associated with the data needed for analytical purposes.

The results obtained by the executable programs of the DACO-MP are printed out in the form of graphics (charts), including peaks (intensity heights), 2θ position and the corresponding d- spacing values.

(III - 9) Data Processing with DACO-MP :-

(III - 9 - a) The peak search :-

Definition and detection of peaks :-

Because of the statistical character of experimental data, the observed intensities, when plotted, do not fall along a theoretical smooth curve, but deviate more or less from it and produce another chaotic diagram .

The DACO - MP has most important parameter of the DACO - MP's peaks search algorithm, which is defined as the length of the interval order to compute its associated polynomial and is called the PKW (peak width).

The second parameter is the threshold (thr) which is defined as the multiple of its standard deviation. The peak width value is given in degrees. The default value of the 'thr' = 1 fits in all the cases.

Experience shows that peaks to be recognized should match the following conditions :

$$\frac{1}{2} FWHM < PKW < 2FWHM$$

Where $FWHM$ is the chord of the peak at the relative intercept level of 0.5. The number of points placed symmetrically around each point is the integer closest to PKW/step size.

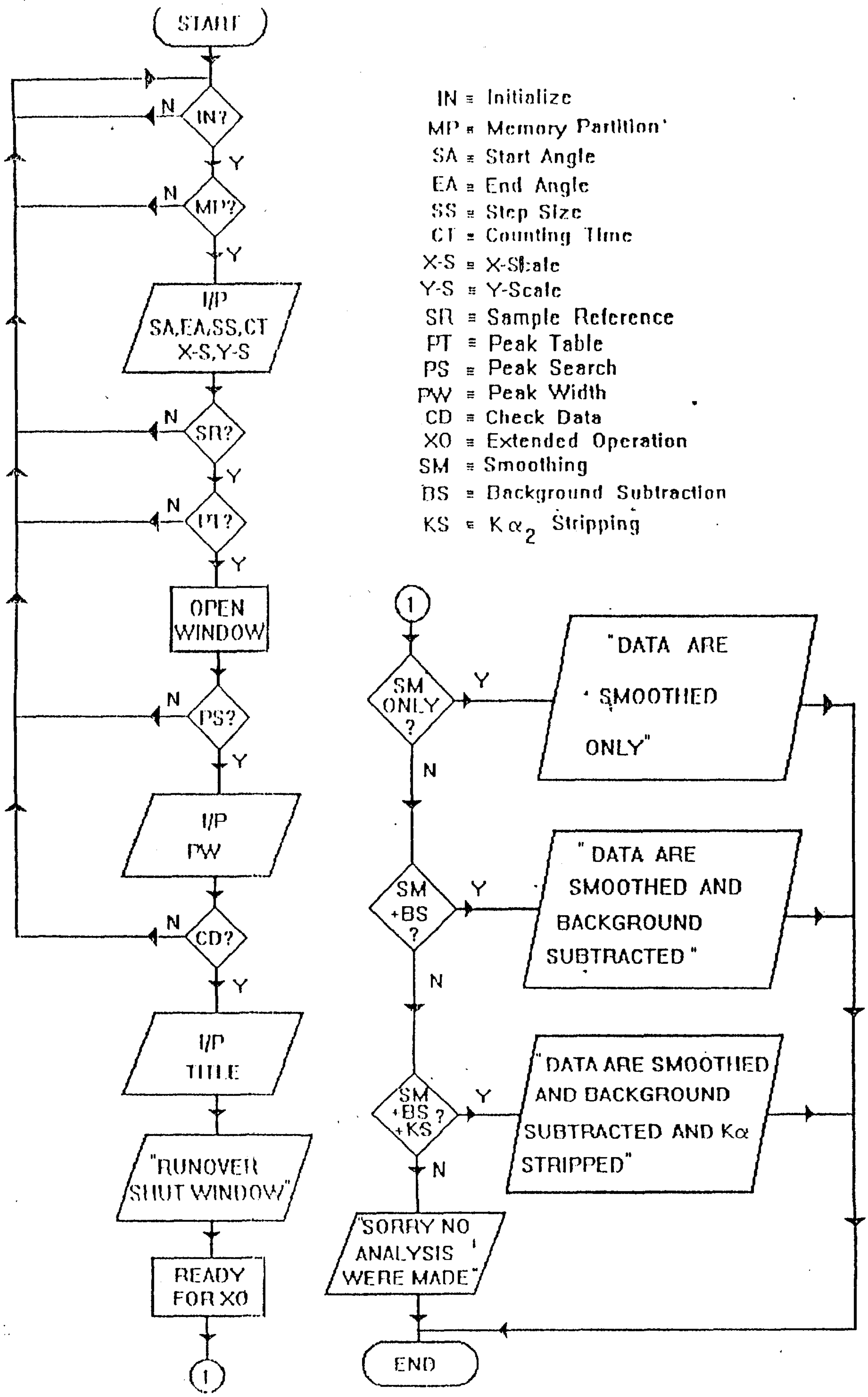

Fig.(III-5) DACO-MP ANALYSIS program flow chart

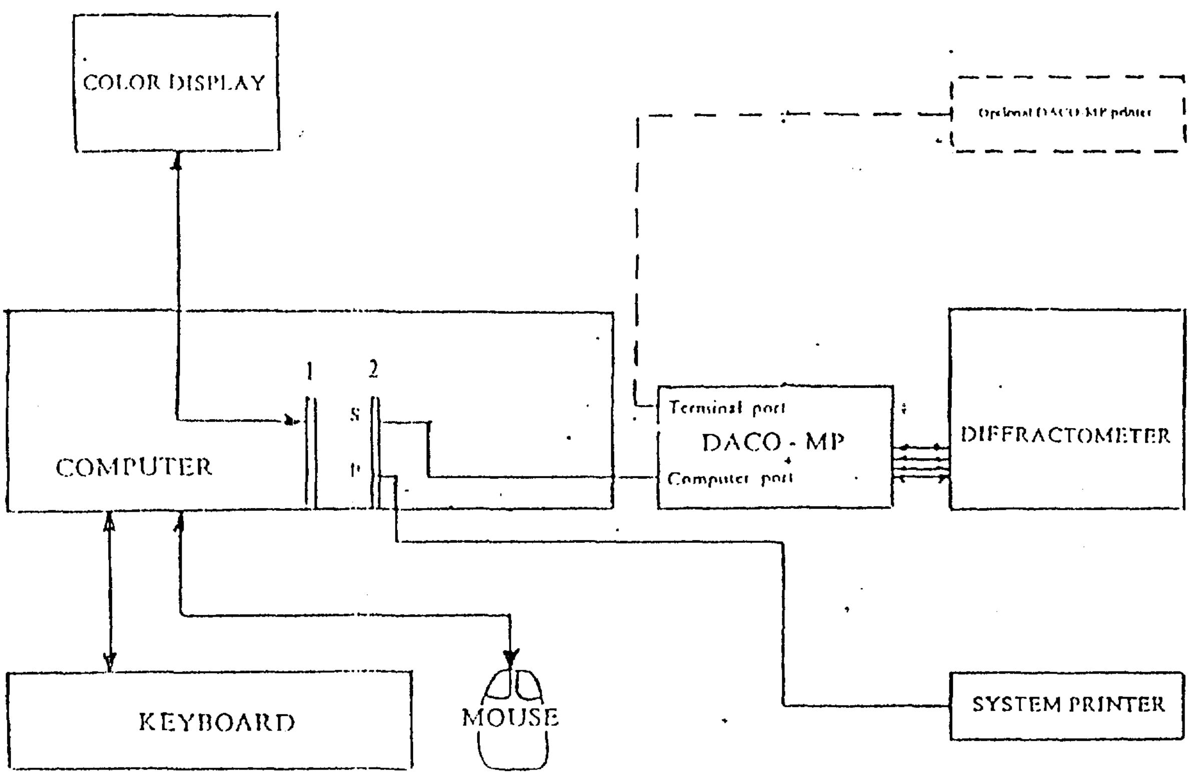

Fig.(III-6) Block diagram of the system in DACO-MP mode

The number of points is the bound to lie between 1 & 15. In some extreme situations, he adaptation of PKW will not be possible because of the inadequacy of the step size.

(III - 9 - b) Extended Operations on Diagrams :

The DACO - MP provides computational operation of the raw data detected experimentally.
The operations are :-

(i) Curve Smoothing :-

The interval for the curve smoothing operation (bit 2) is called SMOI. The number of the points placed symmetrically around each data point is the integer closest to SMOI/step size. This integer is bound to be between 1 and 15 (Getting start with the DACO-MP, Manual V2.1, V2.2 1985).
For each data point, a 3rd degree approximation of the diffractogram is derived from these points, and the central point is replaced by the coefficient of power of the compute apolynomia.

(ii) Continuous back-ground subtraction (bit 4) :-

These coefficient background bkg2 is used to adjust the background subtraction algorith. The equation of the linear by parts, convex, the continuous back ground is given by :-

$$B(2\theta) = Y(2\theta) - bkg2 - [Y(2\theta)]^{\frac{1}{2}} \qquad \text{(III - 9 - 1)}$$

(iii) K alpha 2 Stripping (bit 8) :-

The interval used to control the k. alpha 2 stripping algorithm is called SMO2. This algorithm works on a 3rd degree least square approximation polynomia computed on a fraction of the diffractogram. The length of this fraction is derived from SMO2 as done with PKW and SMO1 for peak search and curve smoothing. The K 2 stripping algorithm is derived from the Rachimer Method.

THIS PAGE IS MISSING IN THE

ORIGINAL DOCUMENT

let:

$$u = \{\omega(\theta) / stepsize\} - k\theta$$

i.e $-0.5 \leq u < 0.5$

then :

$$Y(i) = R[a(i)u^3 + b(i)u^2 + c(i)u + d(i)]$$

Where R is the intensity ratio λ_2 / λ_1
(DACO - MP V2 - 1 USER'S REFERENCE MANUAL)

(III - 10) Data Processing with DIFFRAC - AT V3 - 1 :-

DIFFRAC-AT is an integrated software package for power X-ray diffractometers and provides the measuring routines for the Siemens D5000's and Siements D500's.

DIFFRAC - AT has a list of the following major programmes :-

i) The Graphics evaluation package (EVA. EXE) .

ii)The Plot utilities (PLMON.EXE).

iii)The DIFFRAC - AT integrator (MDMENU.EXE)

iv)The quantitative routines (EDQ.EXE) & (XQUANT.EXE).

v)The date exchange programme (XCH.EXE).

vi)The powder diffraction data base maintenance programme (MAINT.EXE).

vii)The D5000 measuring routines or the D500. This software is not used in this work and the reader is referred to (ELHUSSEIN.1994).

(III -12) Clay mineralogy :-

(III-12-a) Introduction:-

The clay minerals are defined as hydrous aluminum silicate, with fine green size less than 2μ, so they can not be identified by usual optical means. The clay minerals can be identified by special technique such as X-ray diffraction and SEM (Scanning Electron Microscope)(Chamley 1989, Weaver 1989).

III-12-b Clay Minerals Structure:-

Clay minerals are hydrous aluminosilicates, with a sheet or layered crystals structure or they are phyllosilicates, like the micas. The sheets of a clay mineral are of two basic types. One is a layer of silicon-oxygin tetrahedral with three of the oxygin atoms in each tetrahedron shared with adjacent tetrahedral and linked together to form a hexagonal network fig (III-7).

The second type of layer consists of aluminum in octahedral coordination with O^{2-} and OH^{-} ions so that in effect the Al^{3+} ions are located between two sheets of O/OH. The arrangement or the sheet determines the clay -mineral type, as does the replacment of Si and Al ions by other elements. Structurally, the two basic groups of clay minerals are kandite and smectite group.

1. Kandite group:-

Members of the Kandite group have two-layered structure consisting of a silica tetrahedral sheet linked to an alumina octahedral (gibbsite) sheet by common O,OH ions. Replacement of Al to a Si so the stuctural formula is $Al_2Si_2O_5(OH)_4$. The most important members of this group are Kaolinite group.

Kaolinite:

By far the most important, the rare dickite and cacrite, which have a different lattice structure, and hollysite which consist of kaolinite layers separated by sheet of water.Related structurally to kaolinite are alumino-ferrrous silicates bethierine and chamosite and ferrous silicates greenite. Kaolinite has a basal spacing, i.e distance between one silica layer and the next of 7 A^0

2. Smectite group:-

Members of the smectite group have a three layered structure in which an alumina octahedral layer is sandwiched between two layers of silica tetrahedral. This feature of smectites, as a result of which they are often called "expandable clays" is utilized in their X-ray identification (Tucker, 1991).

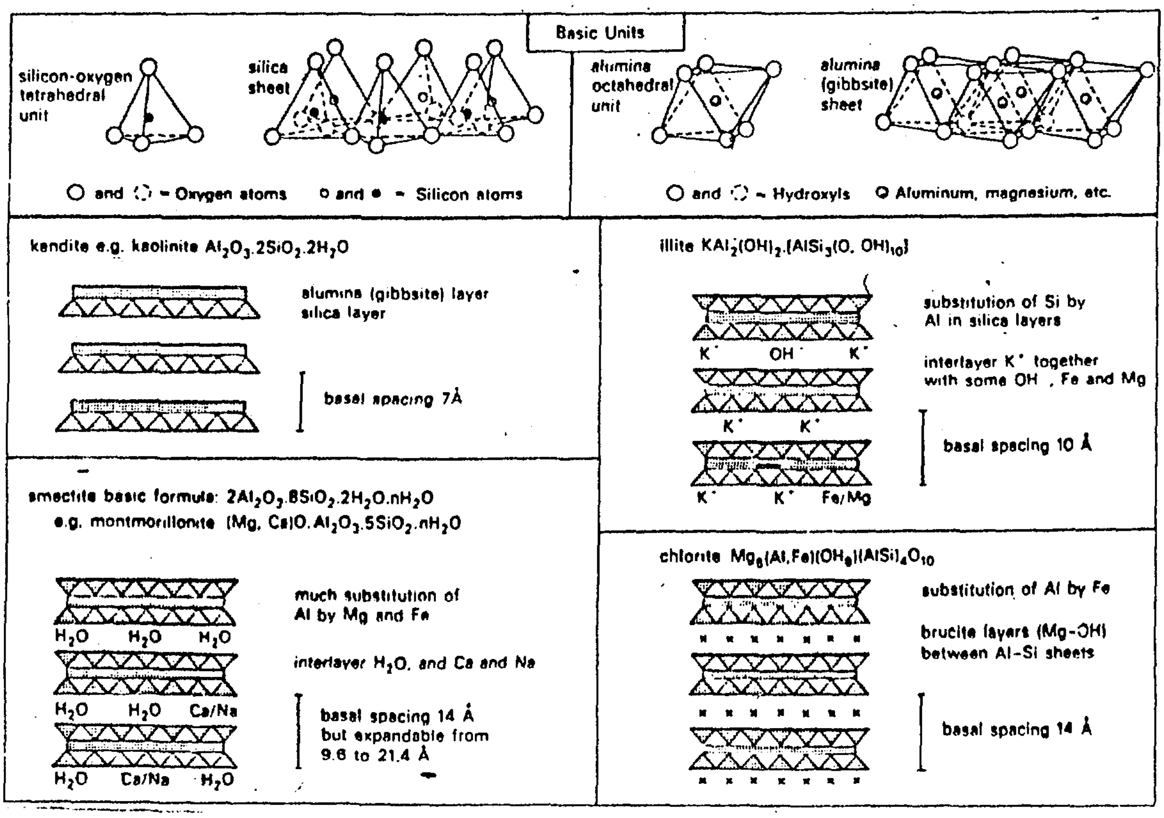

Fig.(III-7) D iagrams illustrating the structure of clay minerals

1. Chlorite:-

Several other hydrous-silicate minerals produced by weathering, maybe grouped with the clay minerals. Important are the chlorite minerals, whose structure consist of mica-like sheets with the composition $[(Mg, Fe)_6(SiAl)_8O_{20}(OH)_4]$ also having the structure of brucite of $[(Mg, Al)_6(OH)_{12}]$.

2. Illite

The most common of the clay minerals in sediments, is related to the mica muscovite. It has a three-layered structure, like the smectite but Al^{3+} substitution for Si^{4} in the tetrahedral layer results in charge which is balanced by potasium ions in interlayer position. The basal spacing is about $10\,A^0$ (Tucker, 1991).

III-11-c Sample Analysis:

A total number of 17 clay samples were selected for analysis by X.R.D.
These samples cover the strata of the north-west of the Sudan. The strata are different in age and depositional environments which range from shallow marine to fluvial environments.

III-12 Sample Preparation & Separation:

1. Each sample was broken to particles of approximately 10 mm size or less

2. The broken sample is placed in distilled water for 2 days.

3 Then the samples were disaggregated carefully in a porcelain mortar .

4. The sample was left for short time in order to allow the settlement of the coarser particles, and then the water containing the fine suspended sediment was put in bucket.

5. The steps number 3 &4 were repeated for several times.

6. If the hydraulic conductivity is found of more than 50 μS/cm distilled water was added until the hydraulic conductivity of about 50 μS/cm was reached.
7. The suspension was centrifuged for 2 minutes under speed of 2000 round / minute (R/M).

8 The suspension which contains the fraction less than 2 micron was filtered out by sucking filter and allowed to dry in the oven at $50c^{\circ}$.

9 From the clay fraction oriented mounts were prepared on a glass slides for X. R. D analysis under dry glycolation and heating conditions.

III-13 Data Collection :-

Data Collection of clay mineral samples :-

These diffraction patterns were obtained for each sample by means of analysis programme written in DACO-MP Language.

This programme reveals output in form of diffractograms and a table including (2θ) position (peak position) in degrees, d-spacing in A^{0}, intensity height in count per sec. and the relative intensity in percentage of the peaks compared to the highest peak that appears in the diffractogram.

The three diffraction patterns were obtained for the samples that were air dried, ethylene glycol solvated and heated as follows :-

1) Air dried treatment :

Each sample was kept in a desicator for 24 hours so as to get rid of water, the air dried were scanned with the parameters adjusted as follows :-

1. End angle 35°.

2. Step size 0.05°.

3. Start angle 5°.

4. Counting time 2 sec.

5. Peak width 0.14°.

6. X-scale 2° per cm.

7. Y-scale 200 Ps per cm (it can be changed according to the intensity height).

2) Ethylene glycol treatment :

Each sample was kept in a descuator for 24 hours, then the scanning was performed with the same parameters as for air dried samples except the starting angle was shifting to 2° so as to identify smectite clays which usually have their d-spacing shifted to lower 2θ position because of the glycolation.

3) Heat treatment :

The sample was heated in a furance to 550°C for 4 hours, then the scanning was performed the same parameters, as the air dried treatment.

CHAPTER IV

RESULTS AND DISCUSIONS

IV-1 Introduction:

This chapter presents the results of clay minerals and chemical analysis of mudstone samples using both XRD &XRF techniques. Moreover the results are interpreted in terms of geological process and other controlling factors.

IV-2XRD analysis of clay minerals

The identification of the clay minerals in this study was done as follows:
The kaolinite has been identified by the presence of $7.1A^0$peak at $12.20(2\theta)$ for basal reflection (001) which is unaffected by ethylene glycol, but destroyed by heating to 550°C.

The smectite has been identified by the presence of $14A^0$ peak for the same basal reflection which expanded to $17A^0$ when glycolated and collapsed to $10A^0$ when heated to 550^0C .

The illite had been identified by the presence of $10A^0$ which is stable at that peak under the three treatments. Table (IV-1) shows the values of the basal reflection in $d(A^0)$ for the clay minerals after the three treatments normal, glycolated and heated (Thoerz,1976).

The clay minerals have been identified qualitatively and semiquantitatively analyzed according to the normalization method.

The diffractogram results for the clay minerals samples are fig (IV-1-23). In each figure letters N, G and H refer to the three treatments used, N for normal (air dried), G for glycolation and H for heated treatments, respectively.

Mineral	Normal (N)	Glycolated(G)	Heated(H)
K	7	7	--
SM	12-15	17	10
I	10	10	10
C	14	14	14

Table (IV-1) Shows values of the basal reflection in d(A^0) for the clay minerals after the three treatments N, G, H

Sample No	Kaolinite % K	Chlorite % C	Illite % I	Smectite % SM
D15	92.07	1.5	1.5	4.09
B5	87.9	----	9.6	2.4
B9	86	5.8	----	7.75
B24	45	20.5	13.7	20.5
B13	87.5	6.2	----	8.7
I	94	2.4	0.6	1.9
B20	45.5	15.2	15.2	24.2
B25	78.5	7.5	3.2	10.7
IIB	91	4.3	1.8	3
B19	84.7	5	4.5	5
4	96.9	----	3.1	----
B8	91.9	----	----	8.9
B10	47.6	15.9	4.8	31.7
8	83.7	4.4	2.2	11.8
B21	79.7	10.2	5.1	51
AII	95	0.99	2	2

Table (IV-I-a) Clay minerals Percentages determination from XRD analysis

Sample No	Quartz Q2	Feldspr F	Geothite G	Hematite H	Mica M	Lepidocrcoite L
D15	(101)	(201)				
B5	(100)	(201)	(110)			(020)
B9	(101)			(110)		
B24	(101)		(110), (111)			
B13	(100), (101)					
I	(101)		(110)			
B20			(110)			
B25	(101)	(201), (202)				
IIB	(100), (101)					
B19		(201)	(040)			
4	(101)		(040)			
B8	(101)		(110)			
B10	(101)	(201), (130)				
8						
B21						
AII						

Tablle (IV-I-b) *hkl* (001) Non Clays

Group Name	Population of octahedral sheet	Mineral Name	Formula
Kaolinites	Dioctahedral	Kaolinite Narcite Dirite Halloysite	$Al_4[Si_4O_{10}](OH)_8$ $Al_4[Si_4O_{10}](OH)_8.4H_2O$
Smectites (Swelling Clays)	Dioctahedral	Montmorillonite Beidellite Nontronite	$0.33M^*(Al,Mg)_2[(Al,Si)_4 O_{10}](OH)_2.nH_2O$
Leptochlorites Chlorites Orthochlorites	Trioctahedral -Dioctahedral Trioctahedral Trioctahedral	Pennite Clinachlore	$(Mg,Fe)_5Al[Al\ ,Si_3O_{10}]\ (OH)_8$
Illite		Illite Pinnite Phengite	$NaAl_2\{AlSi_3O_{10}\}(OH)_2$
Feldspar	Alkalidespar Series		$(K,Na)\{AlSi_3O_8\}$
Quartz	Framework sil-icates	Silica minerals	SiO_2

Table IV-II Classification of layer Silicates

The * symbol on peak indicates that the interpolation program that computes the accurate 2Θ maximum value has failed.
The clay minerals samples percentages were calculated as in table (IV-1-a) and the non clay minerals has shown in table (IV-1-b).
While table (IV-2) shows more descripitve result of unknowns.

As can be seen from the diffracograms and table (IV-1-a) the clay minerals identified include in decreasing abundances of kaolinite, smectites , chlorite and illite. Other non clay's recognised are quartz and feldspars.

In almost all samples except 2 samples kaolinite dominates with percentages ranging between 78% - 96%. In the remaining 2 samples kaolinite ranging between 45% - 47%.

Among other clay minerals smectite comes second in abundance, where 6 samples range between 10% - 24%. Chlorite and illite show the lowest abundances.

The high kaolinite content associated with rather less smectite, in these mudstone samples, most probably indicates intensive and advanced stage of chemical weathering and leaching , operated under warm and humid climatic conditions (Chamley, 1989). Therefore , kaolinite could be of detrial origin mostly inheirted from parent rocks subjected to weathering under the humid climate (Millot, 1970).

The relative increase of smectite may reflect that the humid climate was interrupted by dry period , or indicates environmental change from continental fluvial to marine environment. Moreover, the increase of chlorite and illite percentages may suggest physical weathering directly from the parent rock or early stage of the clay minerals formation (Chamley, 1989). Given the environmental (fluvial, marine) and climatic condition of NW Sudan in the past geological time, one cannot exclude fully that some of the clay minerals could have been produced in part by neoformation and/or transformation (Tucker, 1989).

IV-3 XRF Chemical Analysis:

XRF technique is used to determine the elemental chemical composition of mudstone samples investigated by XRD. Elements determined includes both major and trace elements.

The tables(IV-24-33) show the spectra fitted with tables showing the concentration in ppm percentages. XRF results show that the concentration of both major and trace elements varies among some of samples studied, for instance, this variation is noted clearly between kaolinite-rich and smectite-chlorite -illite-rich samples, in the concentration of major and trace elements.

The variation in element concentrations reflects the clay minerals composition of these samples which are controlled by the geology and the intensity of chemical weathering and leacging under the prevailing climatic condition (Chamley, 1989). Moreover the physiochemical behaviour of these elements might also be responsible for that variation (Manson, 1952). For example, it is known that the kaolinite is characteristic of acid soil where leaching is intensive. In contrast, smectite, illite and chlorite indicate limited intermediate stages of leaching. Moreover, the degree of leaching and pH-Eh are both largely determined by climate, are the two main factors controlling clay mineral formation of the host rock. Thus composition of the host rock or sediment is also important (Tucker, 1991).

B15,N,0.14

THU 29-FEB-96 12:29: 3

PHYSICS DEPT. U. OF K., XRD GROUP

Anode : Cu K1+2, Lambda : 1.54060, Lambda2 : 1.54442

M. time: 2.000, Step size: 0.050

Start at 2Theta 5.000 Theta 2.500

2Theta - Scale

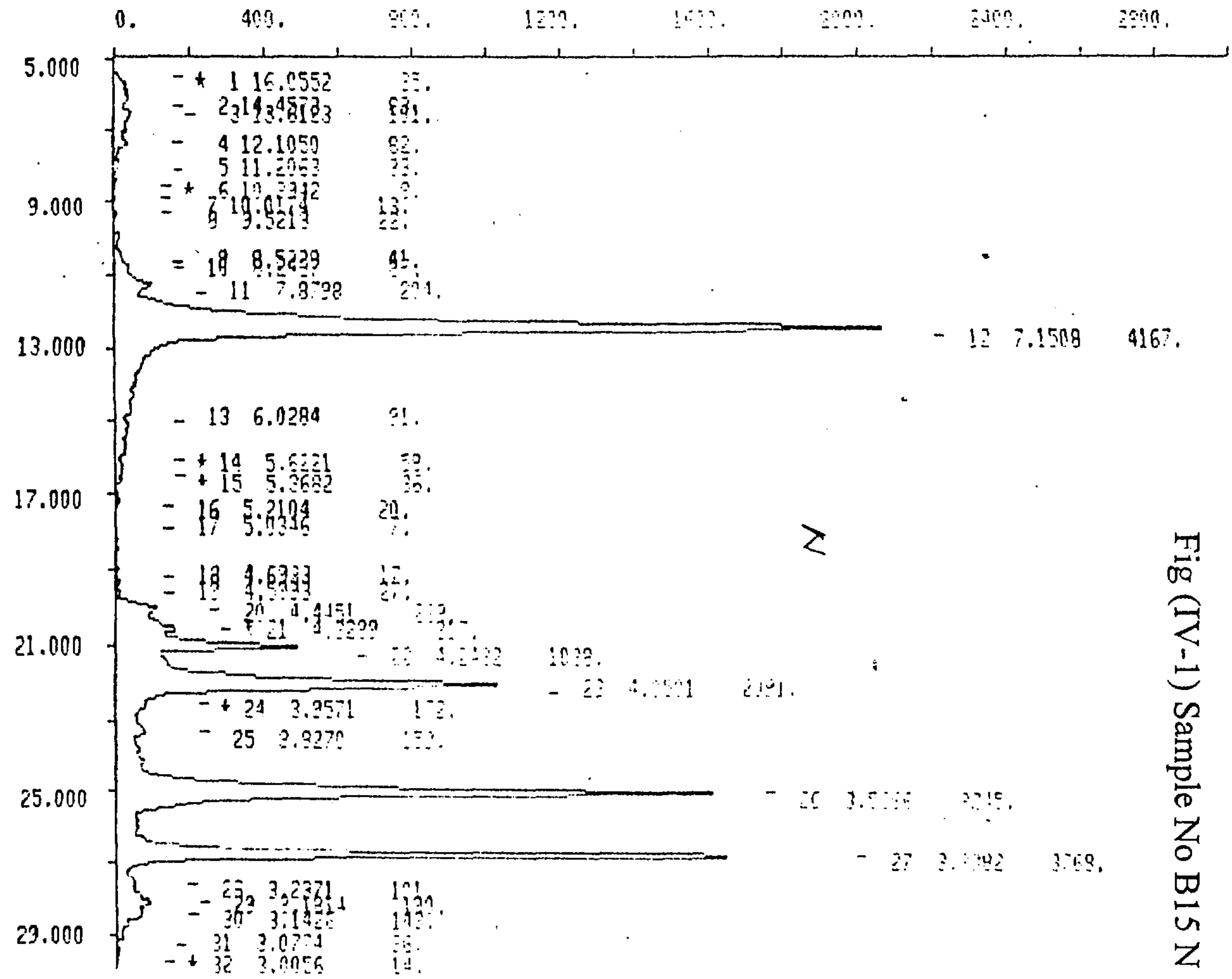

Fig (IV-1) Sample No B15 N

B15,G,.14
FRI 11-AUG-95 11:52:56
PHYSICS DEPT. U. OF K., XRD GROUP
Anode : Cu K1+2, Lambda : 1.54060, Lambda2 : 1.54443 (0.500)
M. time: 2.000, Step size: 0.050 [SS]
Start at 2Theta 2.000 Theta / 1.000
2Theta - Scale

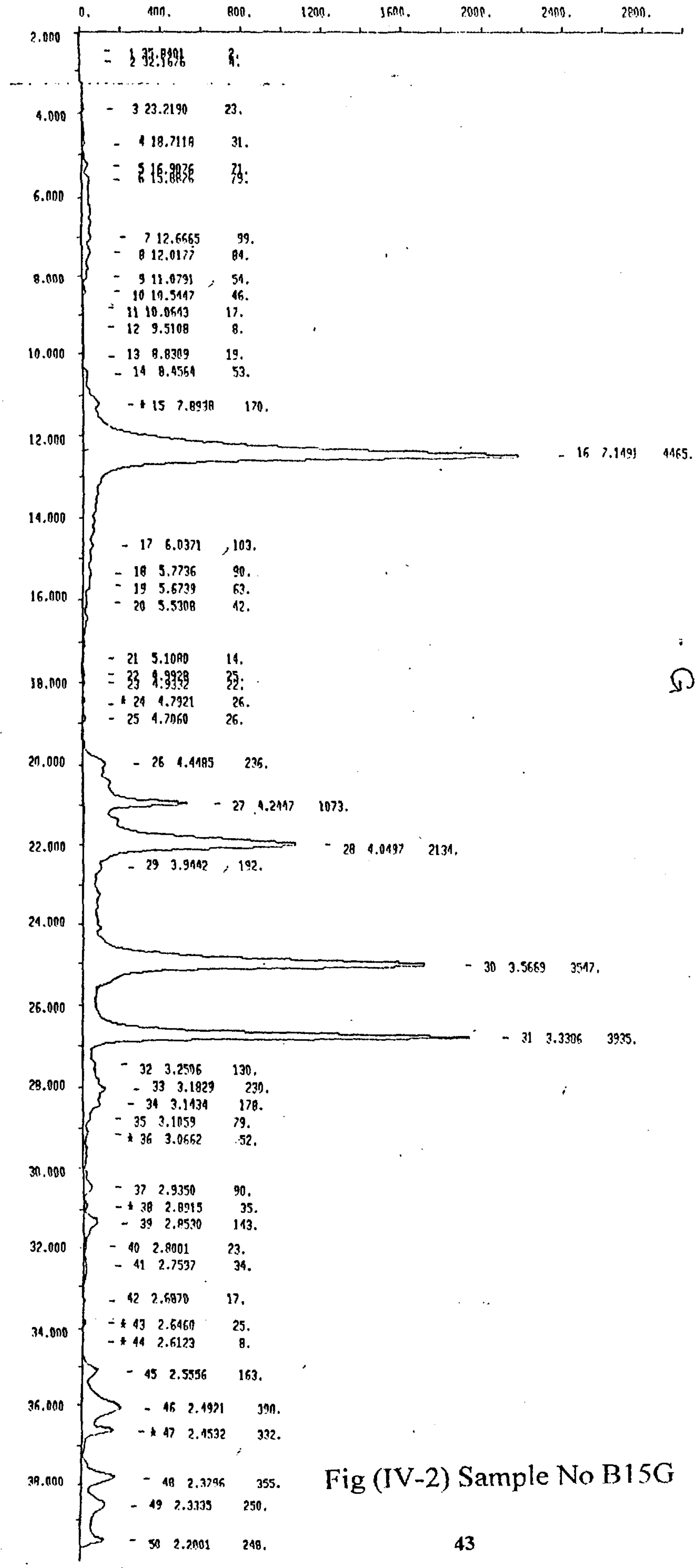

Fig (IV-2) Sample No B15G

B5,N,0.14+
TUE 5-MAR-96 13: 8: 2
PHYSICS DEPT. U. OF K., XRD GROUP
Anode : Cu K1+2, Lambda : [illegible], Lambda2 : [illegible]
M. time: 2.000, Step size: [illegible]
Start at 2Theta 5.000 Theta [illegible]
2Theta - Scale

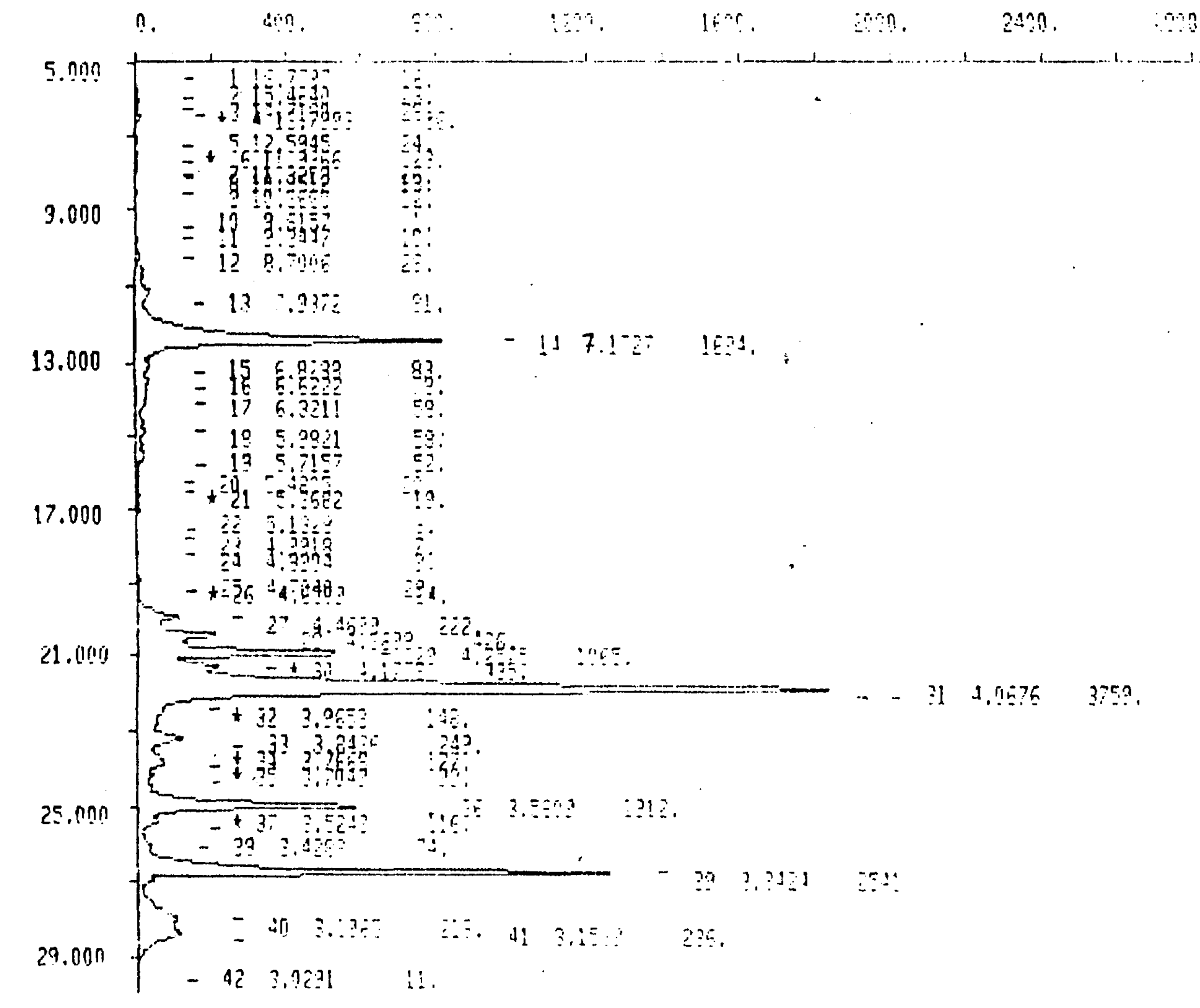

Fig (IV-3) Sample No B5 N

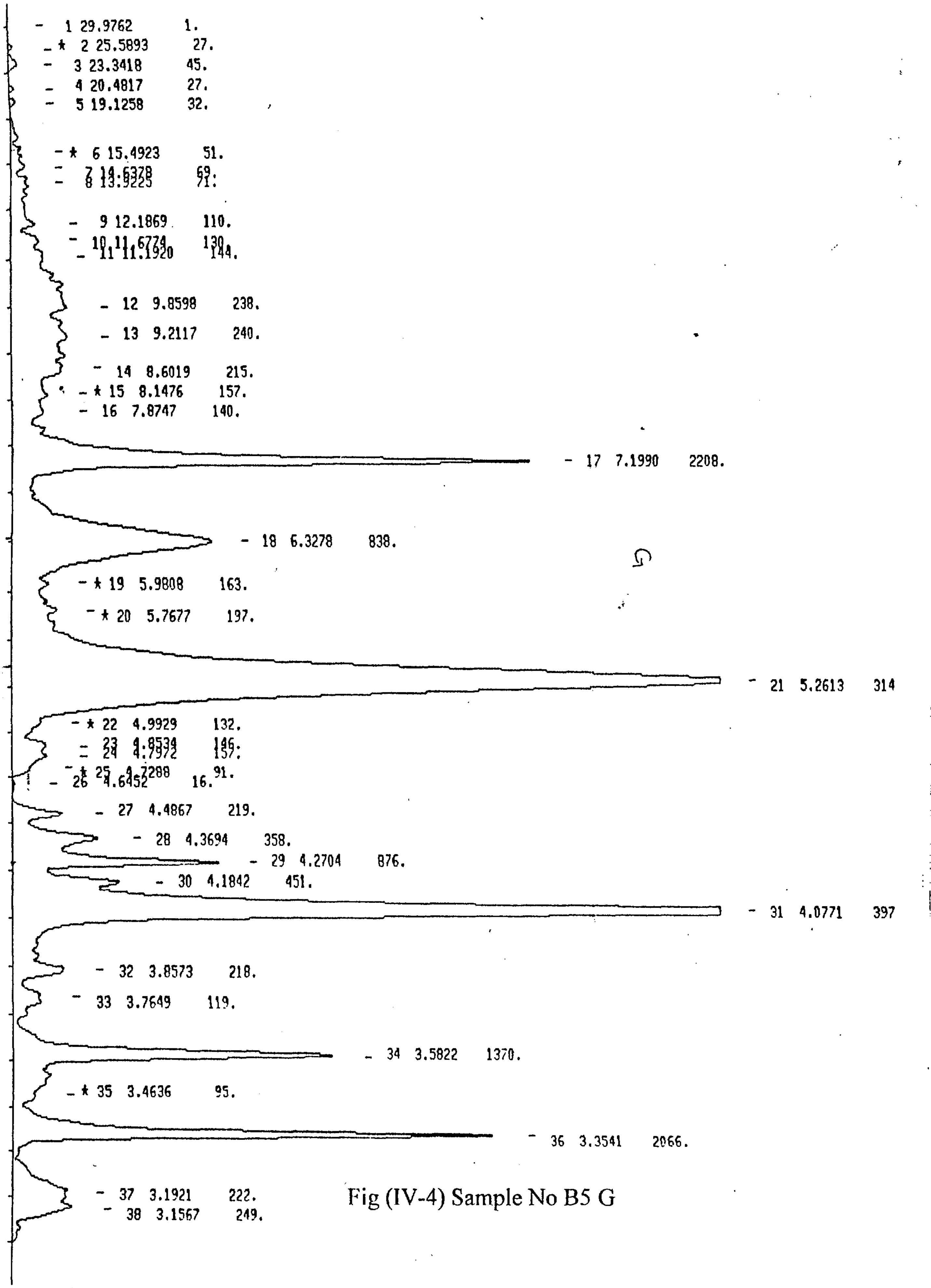

Fig (IV-4) Sample No B5 G

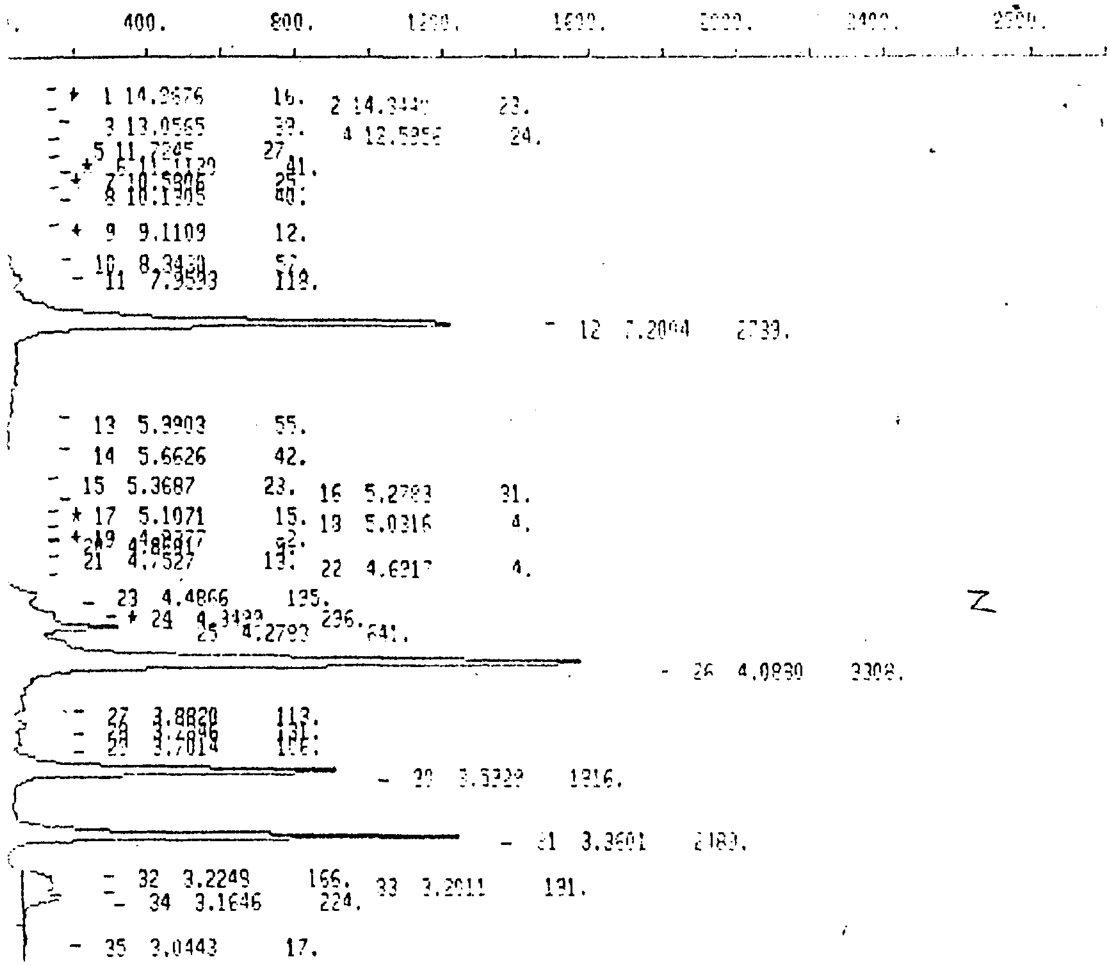

Fig (IV-5) Sample NoB9 N

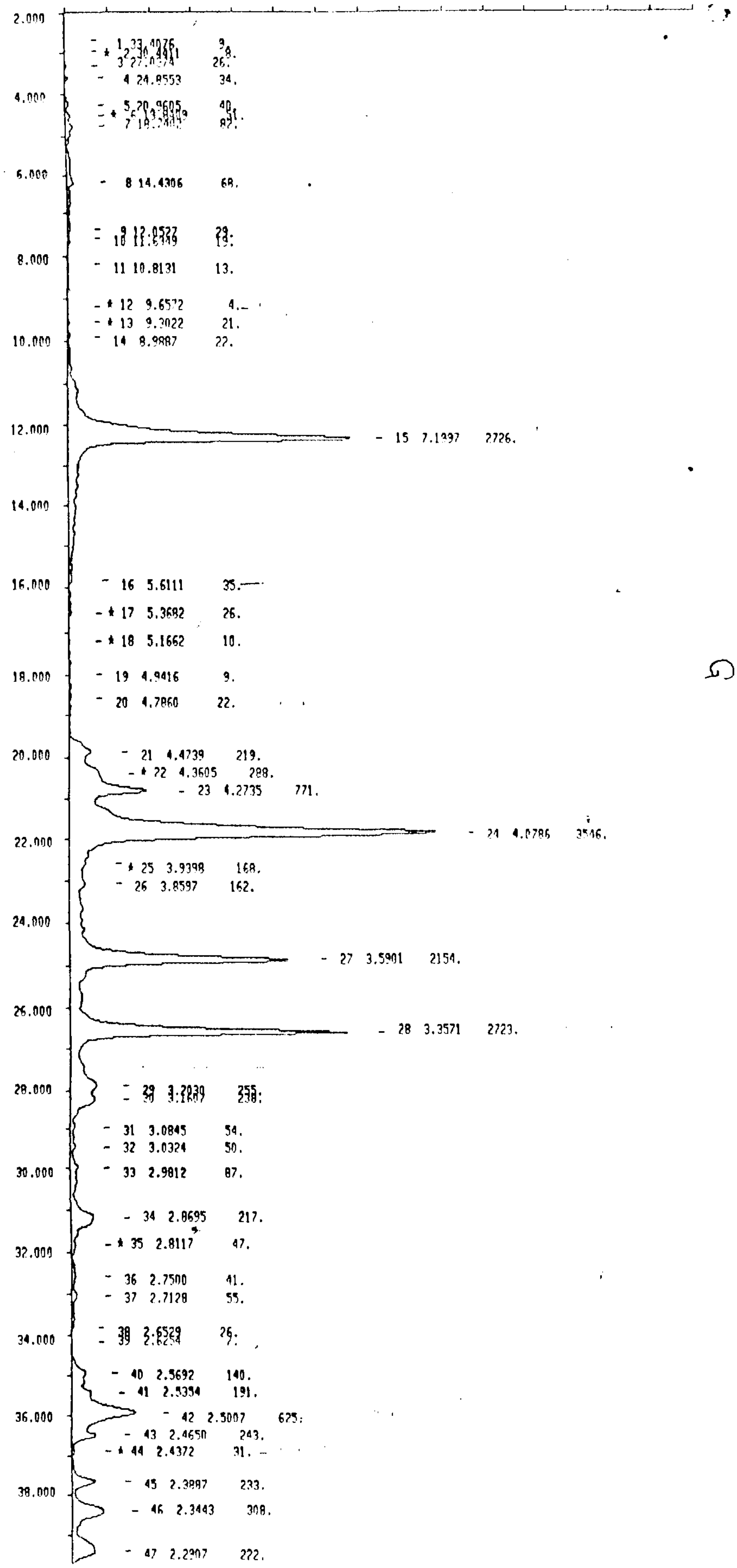

Fig (IV-6) Sample No B9 G

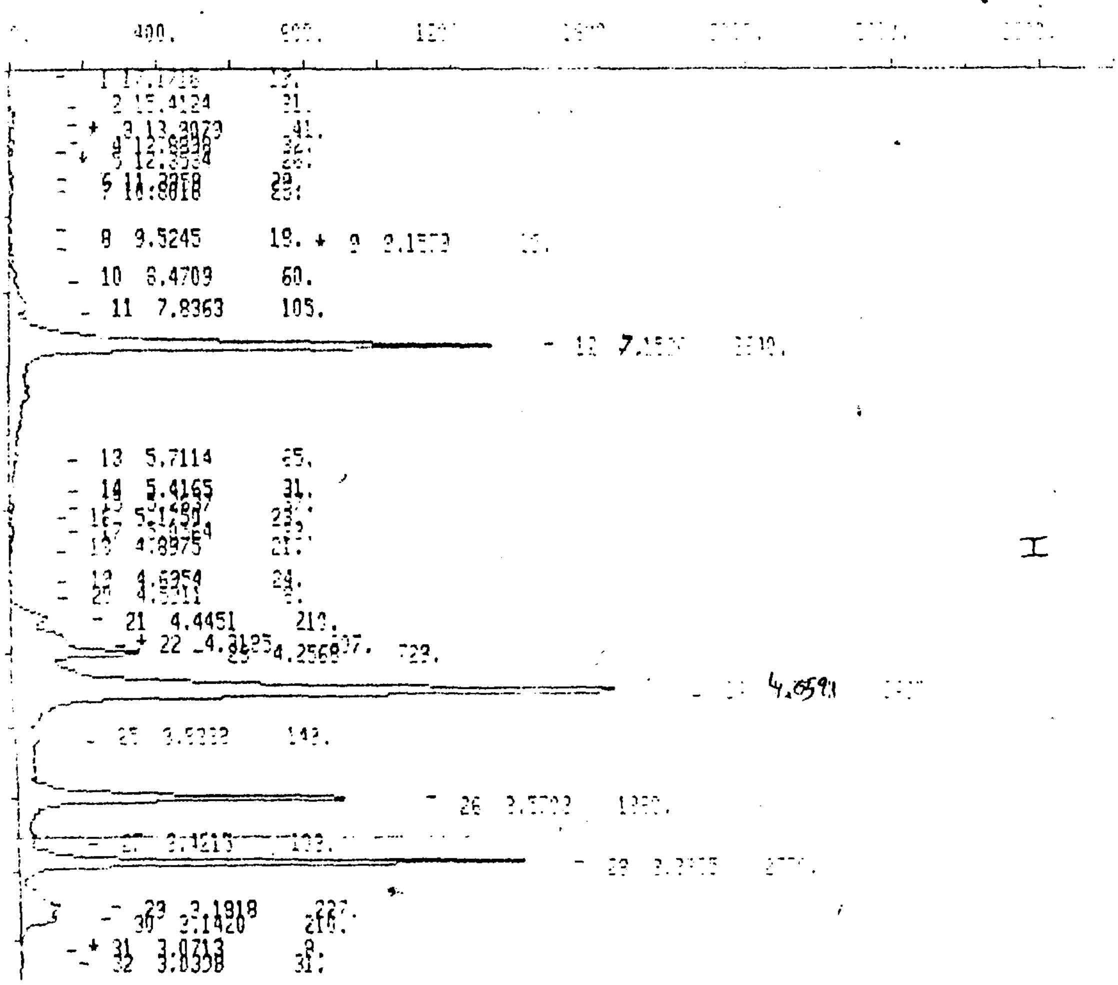

Fig (IV-7) Sample No B9 H

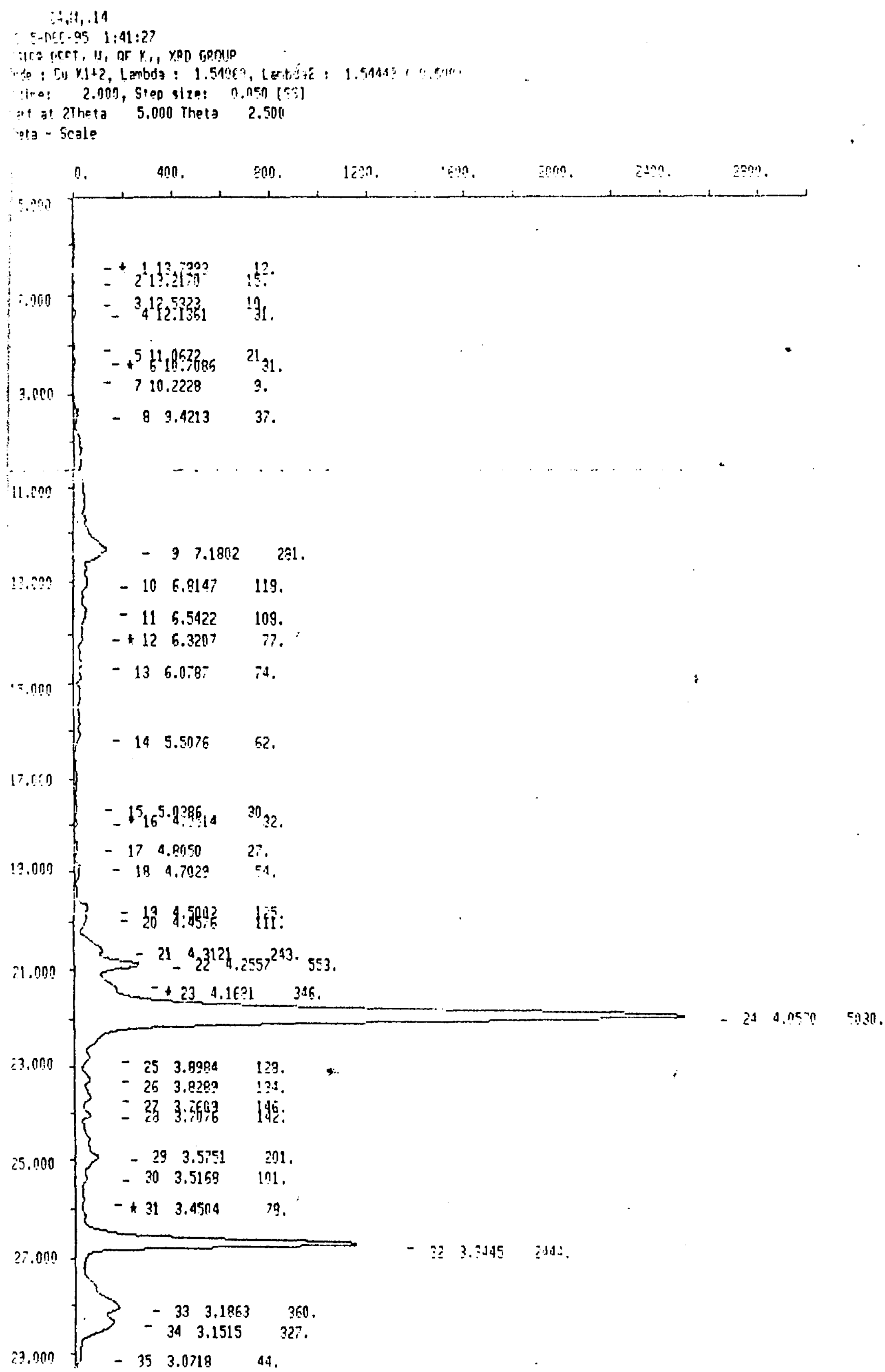

Fig (IV-8) Sample No B24 N

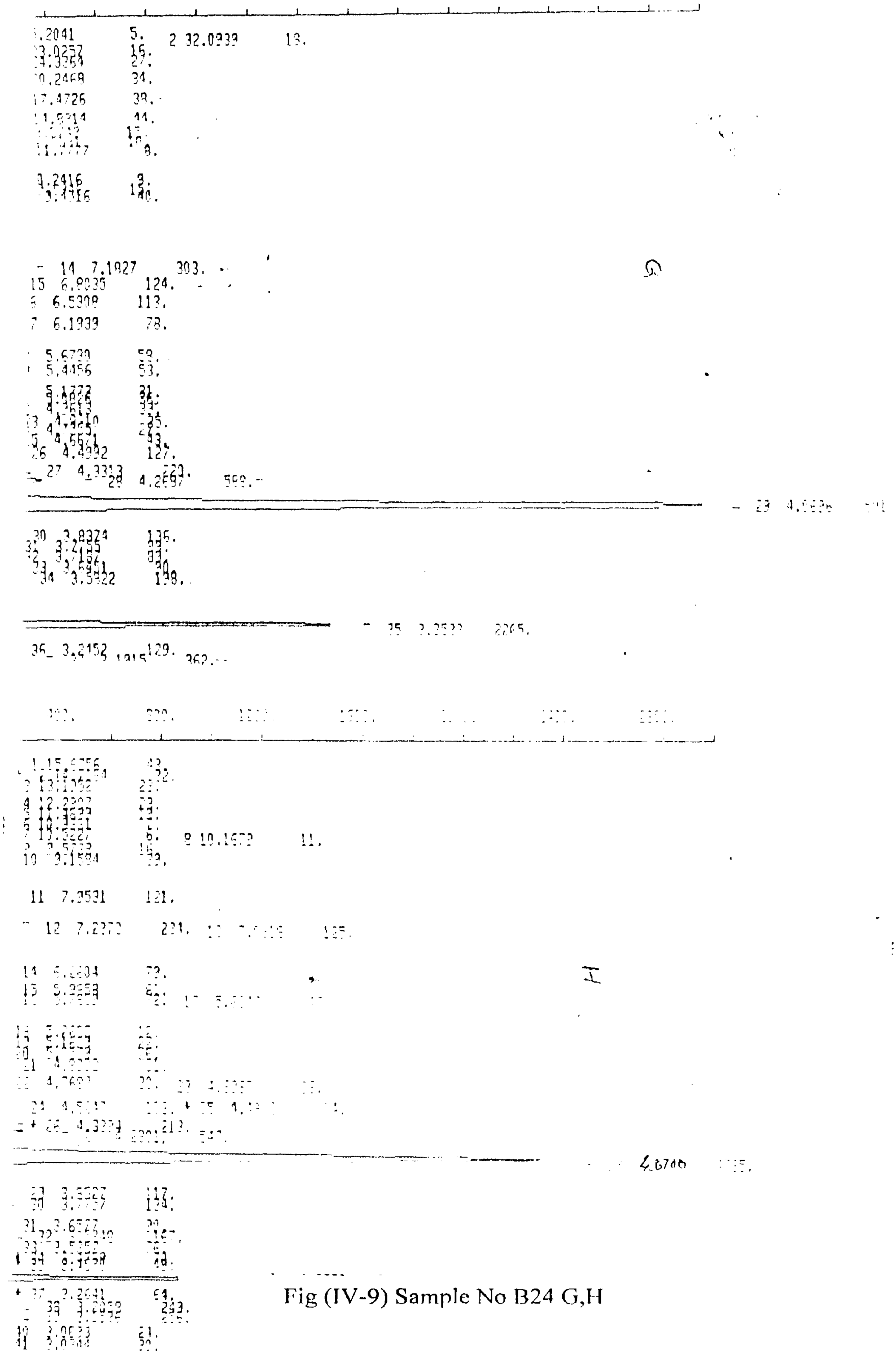

Fig (IV-9) Sample No B24 G,H

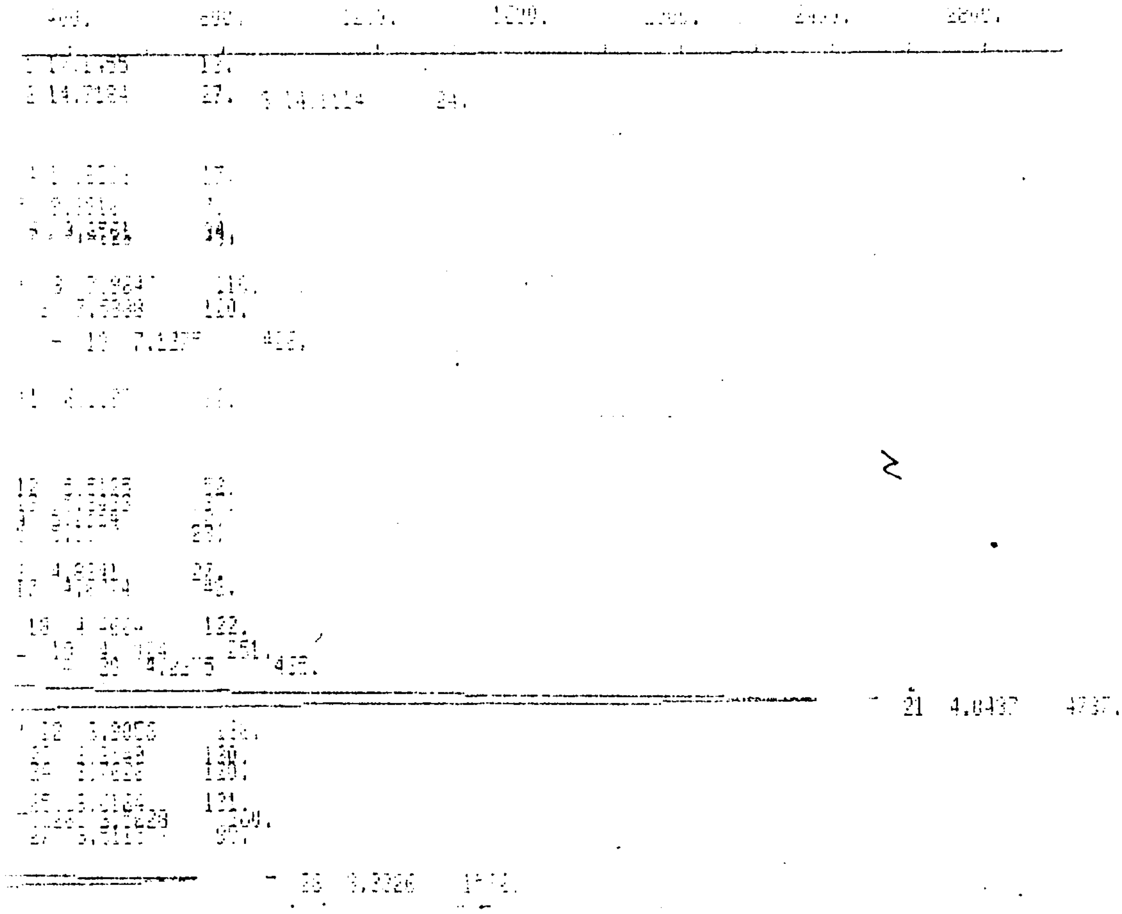

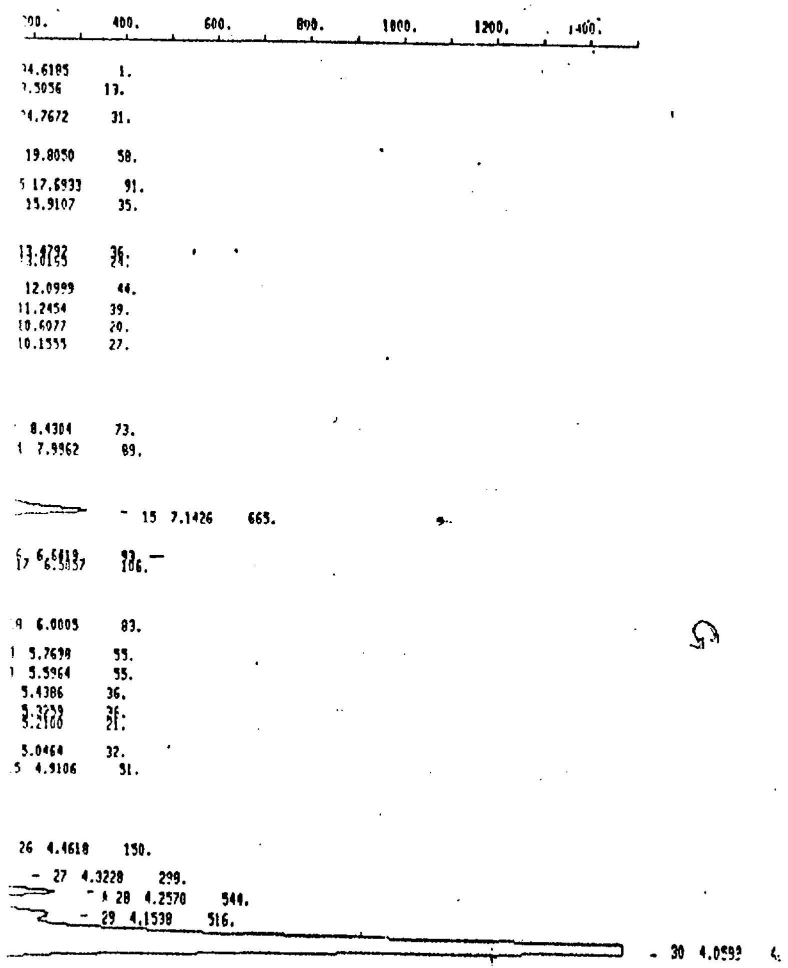

Fig (IV-10) Sample No B13 N,G

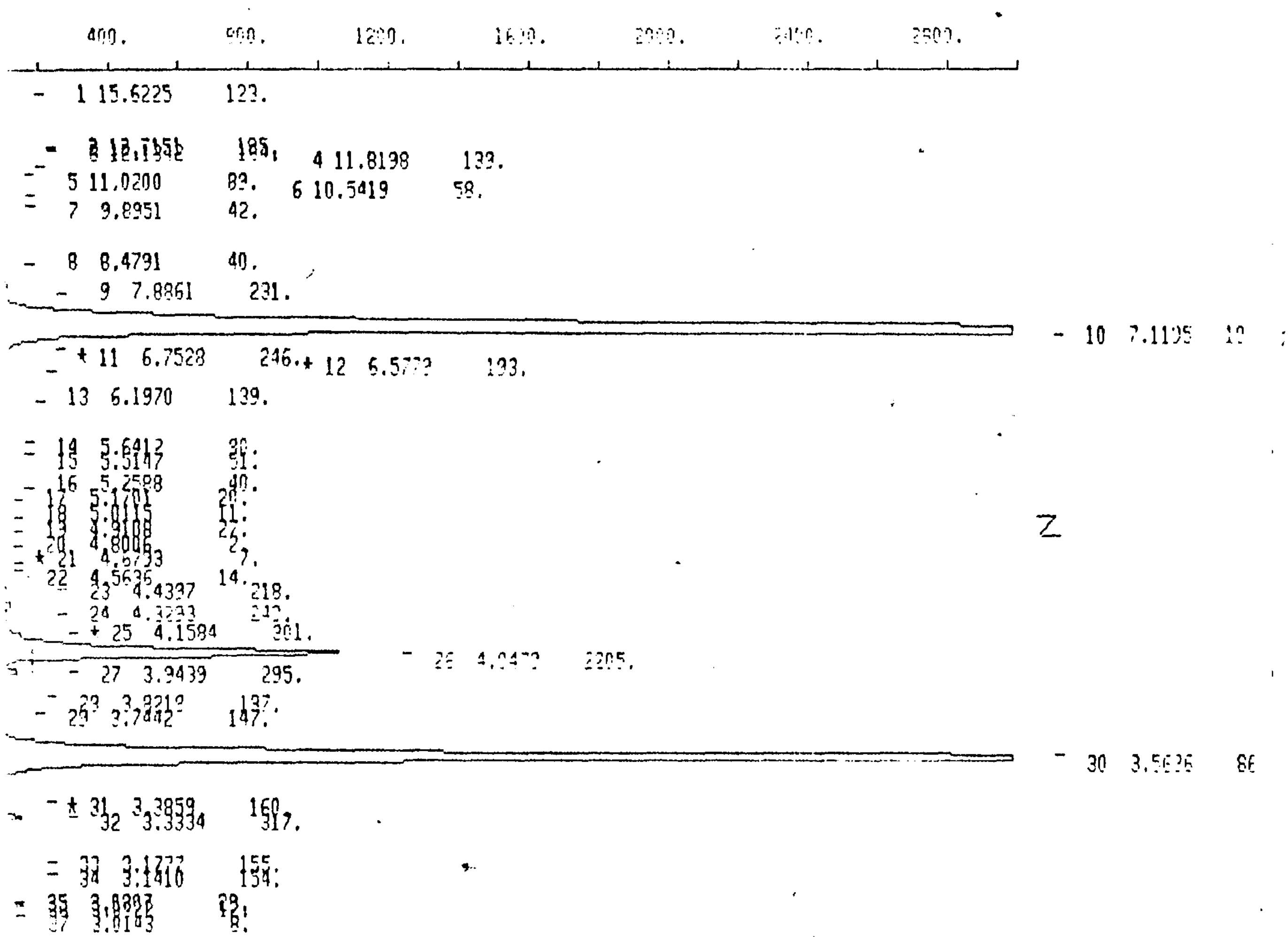

Fig (IV-11) Sample No I N

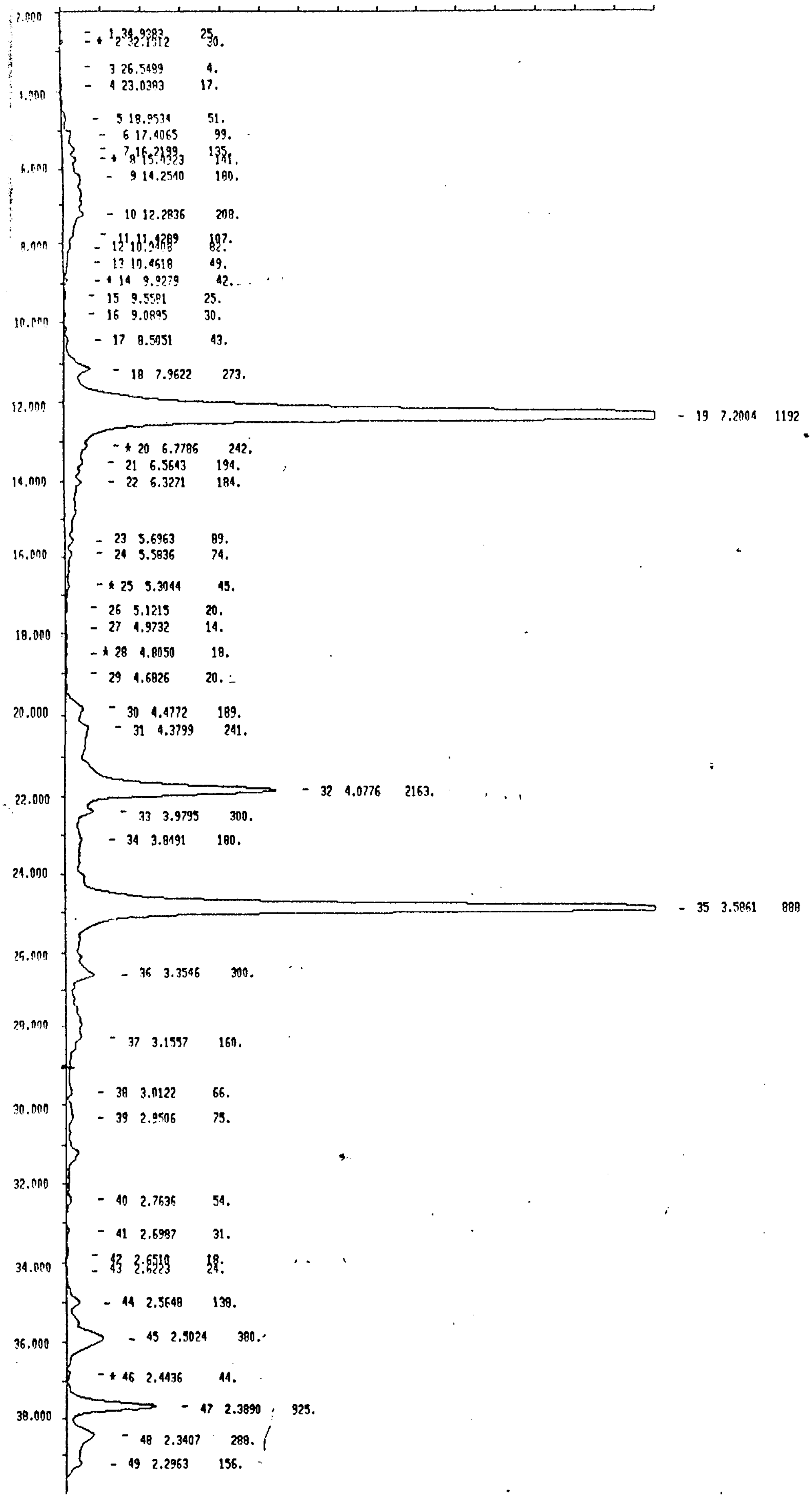

Fig (IV-12) Sample No I G

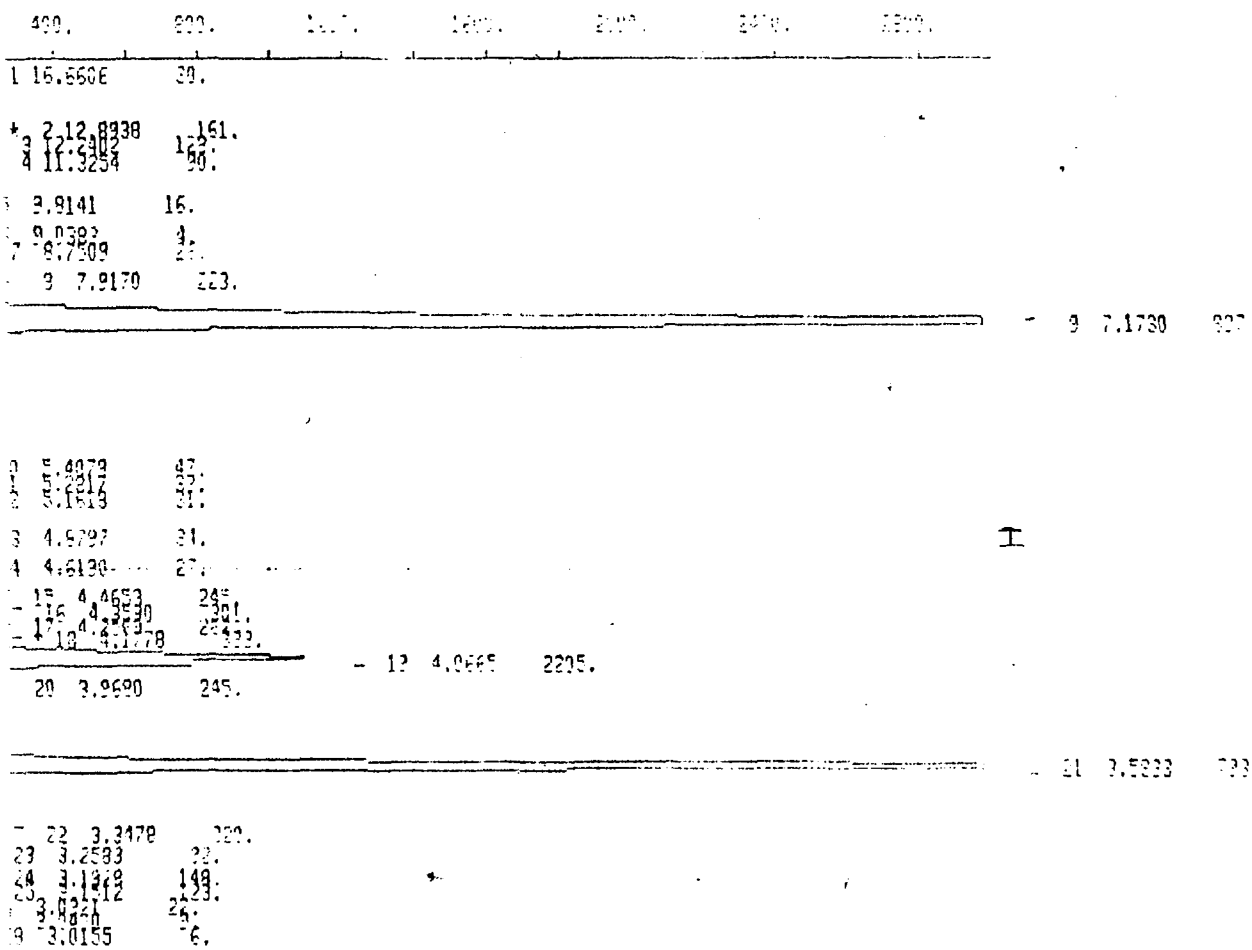

Fig (IV-13) Sample No I H

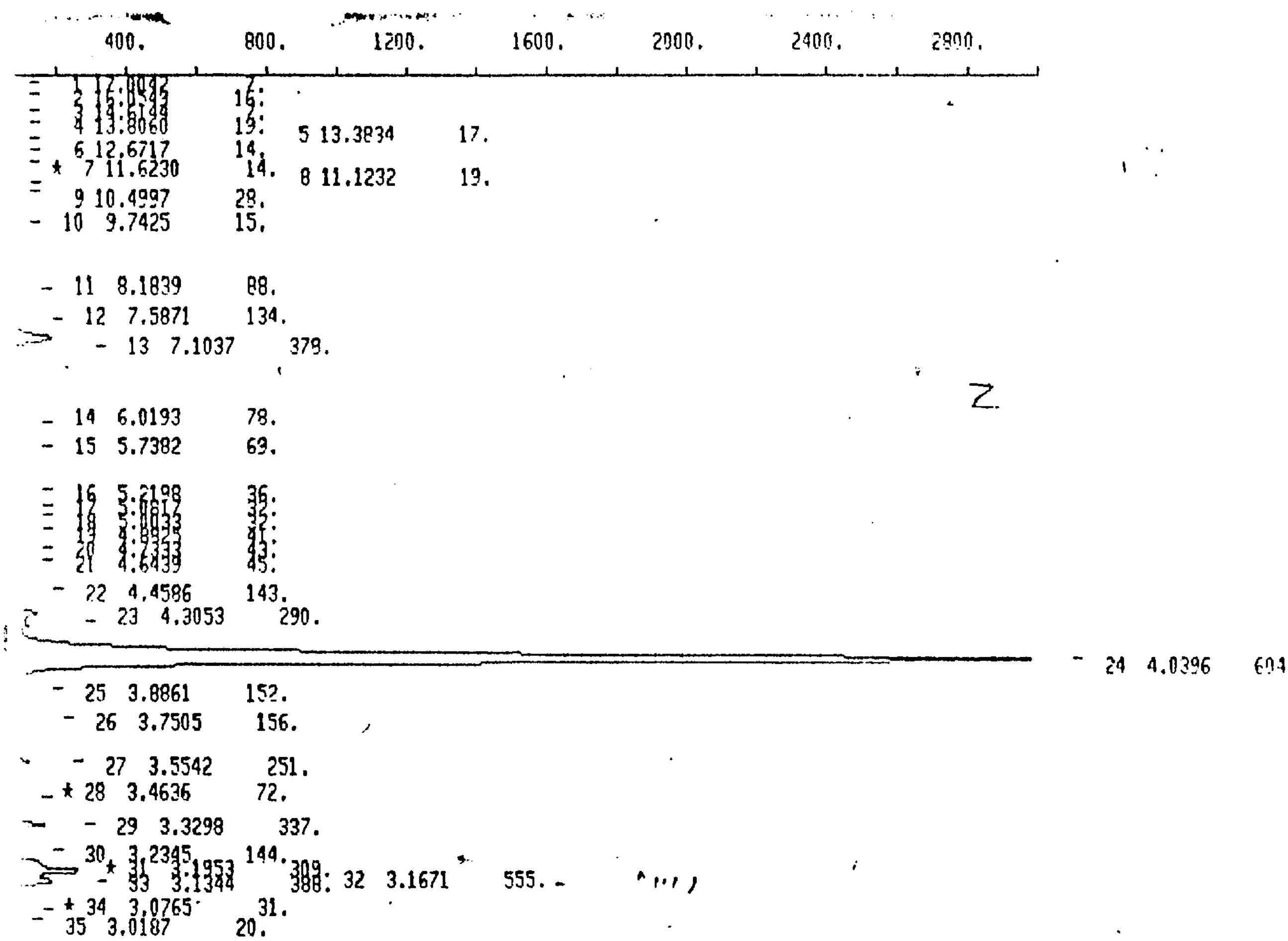

Fig (IV-14) Sample No B20 N

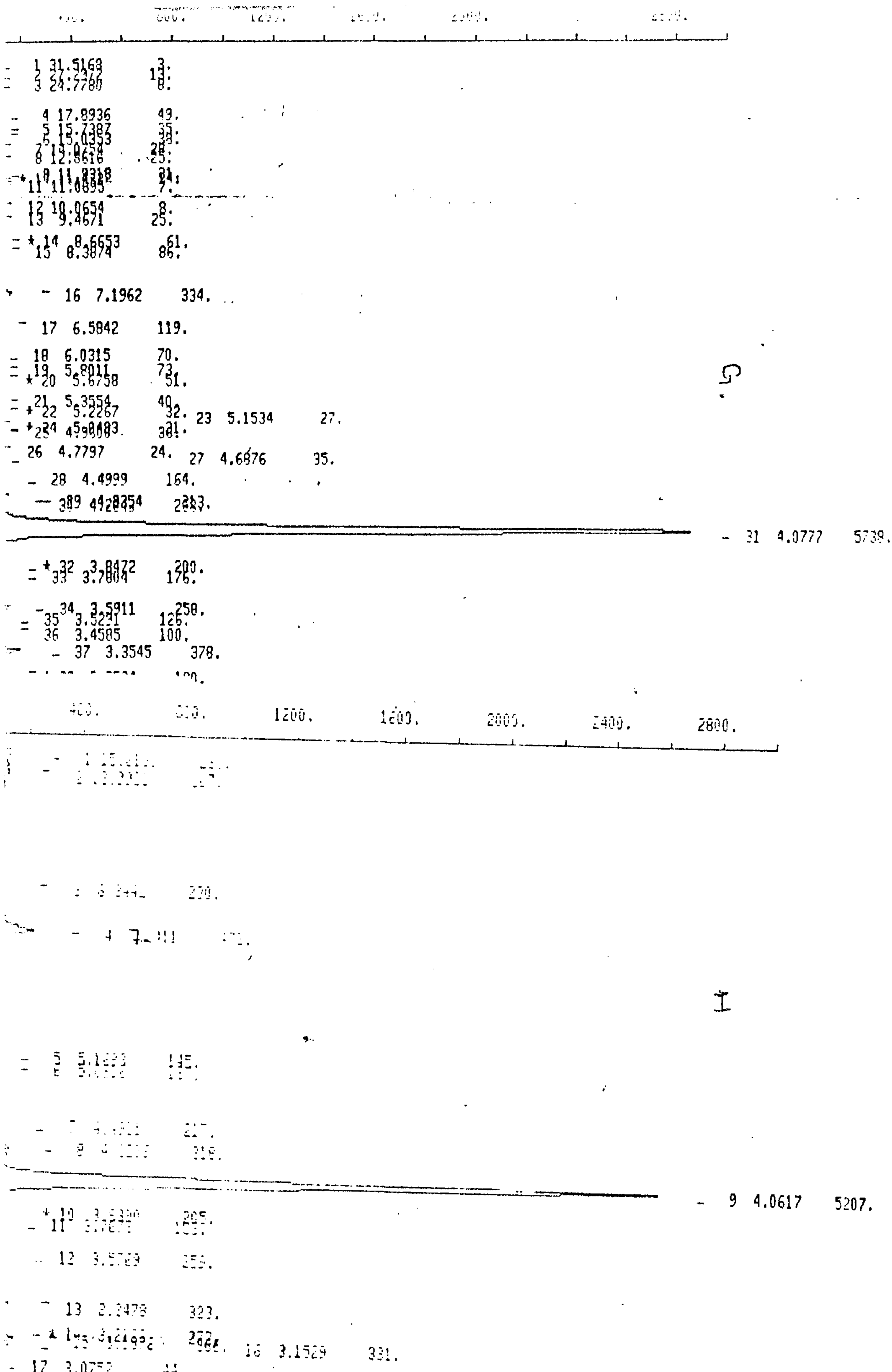

Fig (IV-15) Sample No B20 G,H

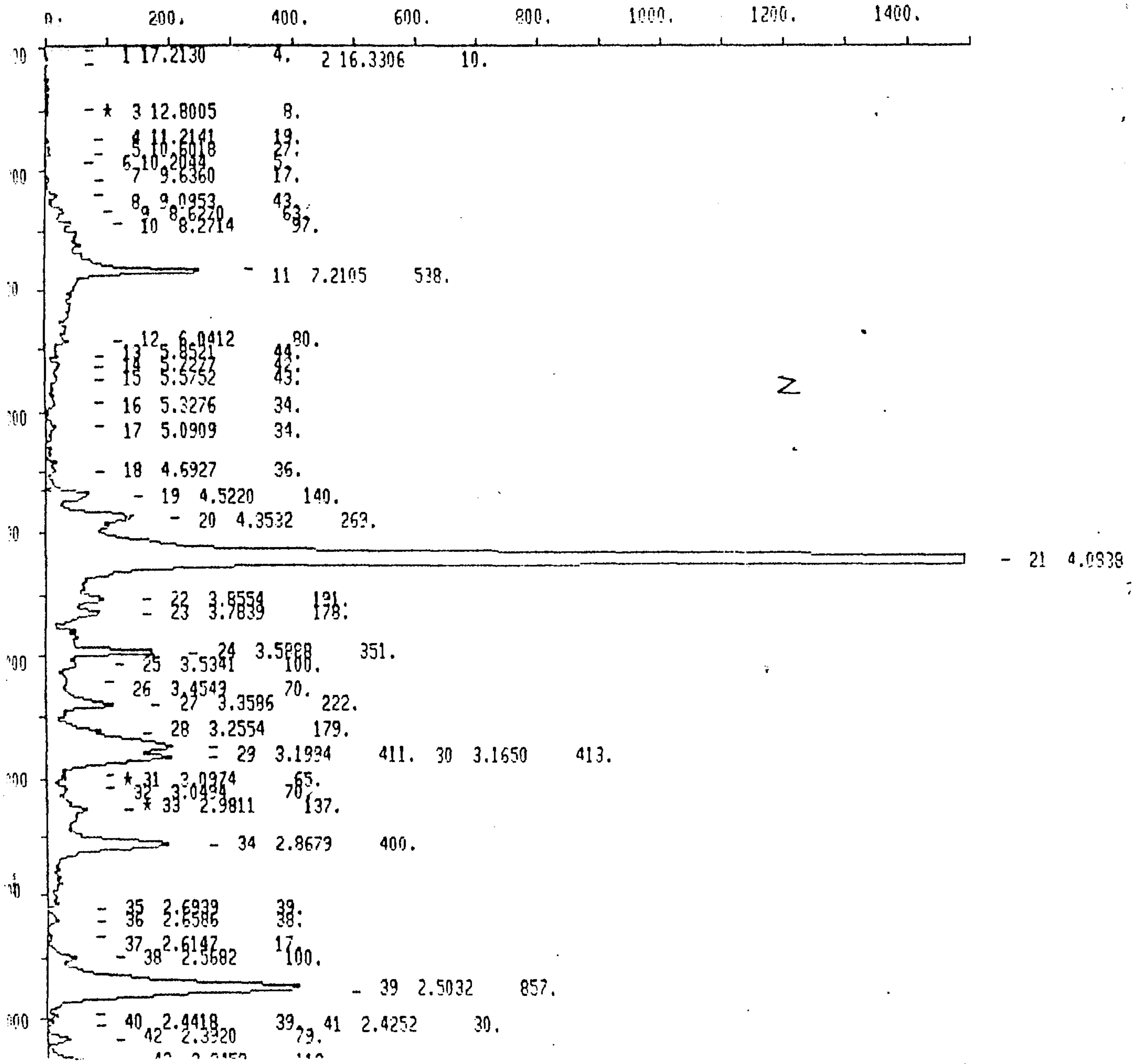

Fig (IV-16) Sample No B19 N

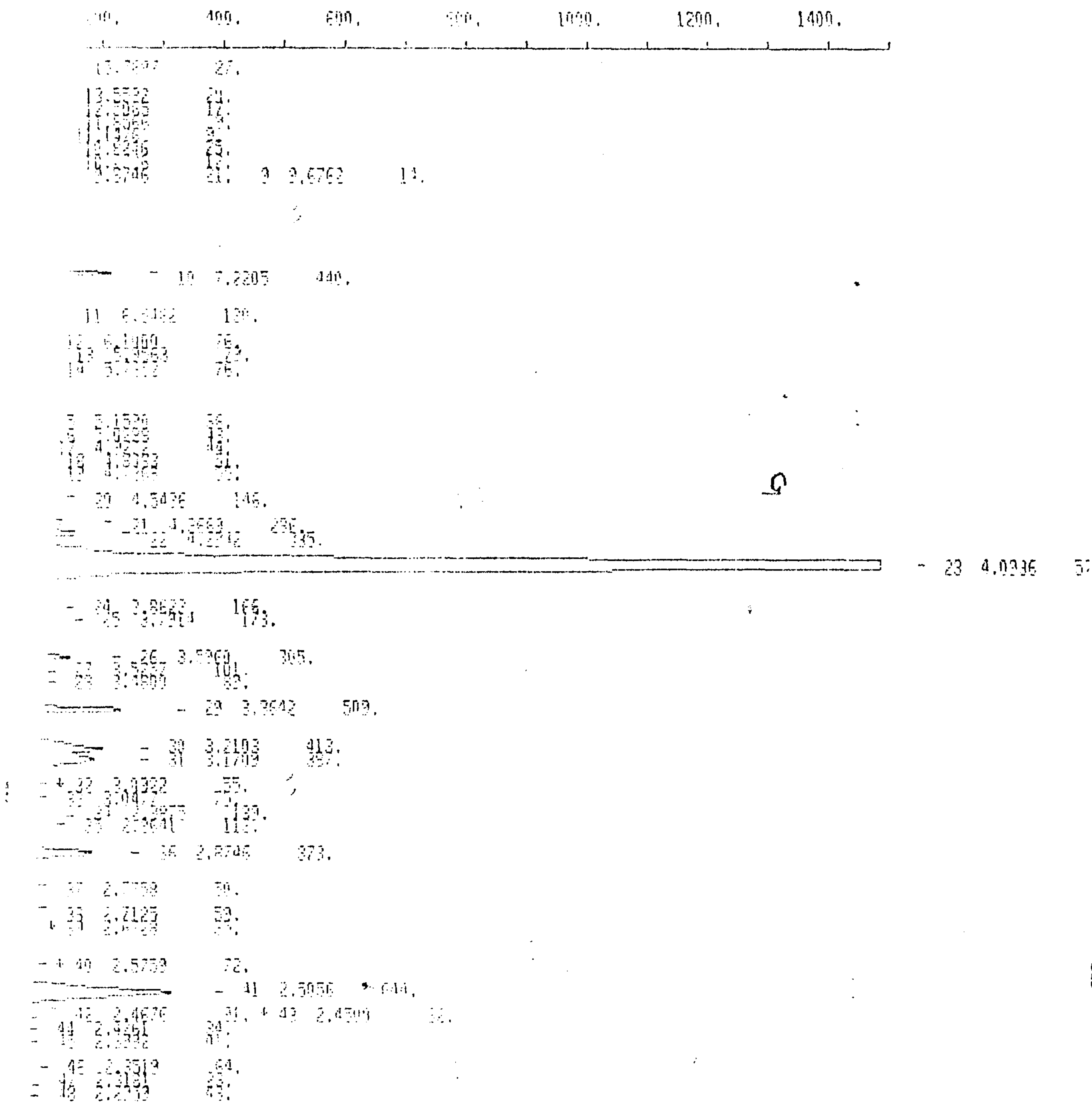

Fig (IV-17) Sample No B19 G

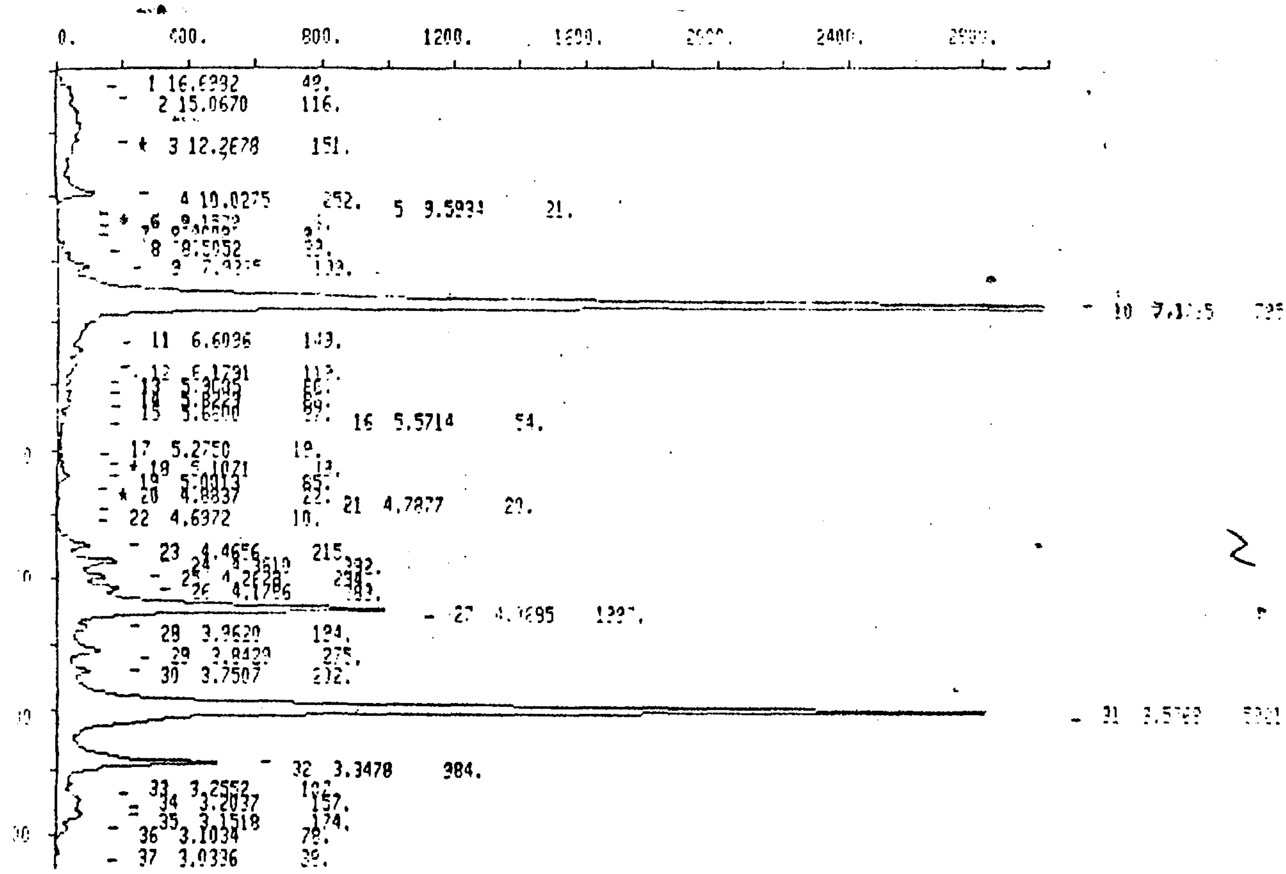

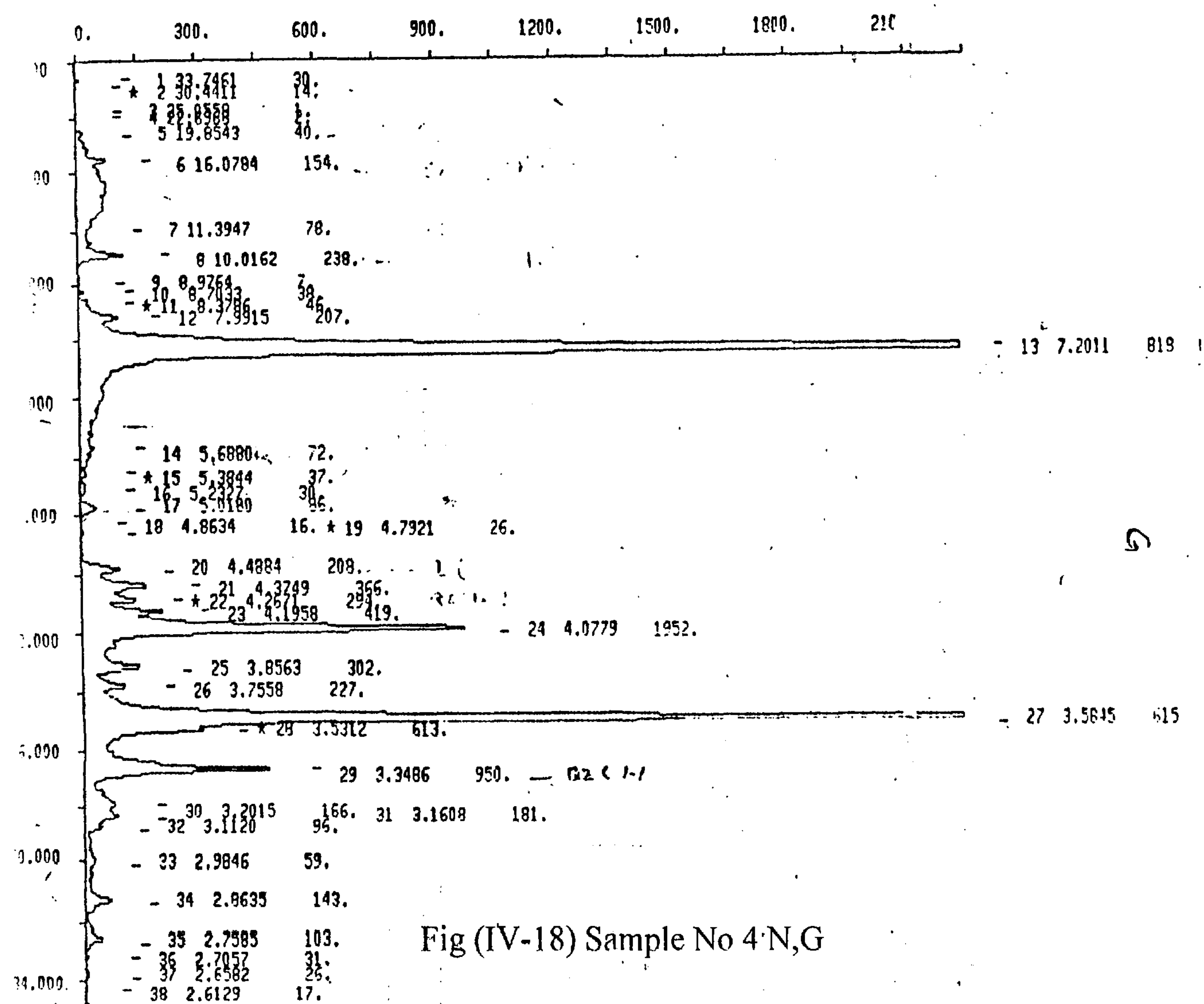

Fig (IV-18) Sample No 4·N,G

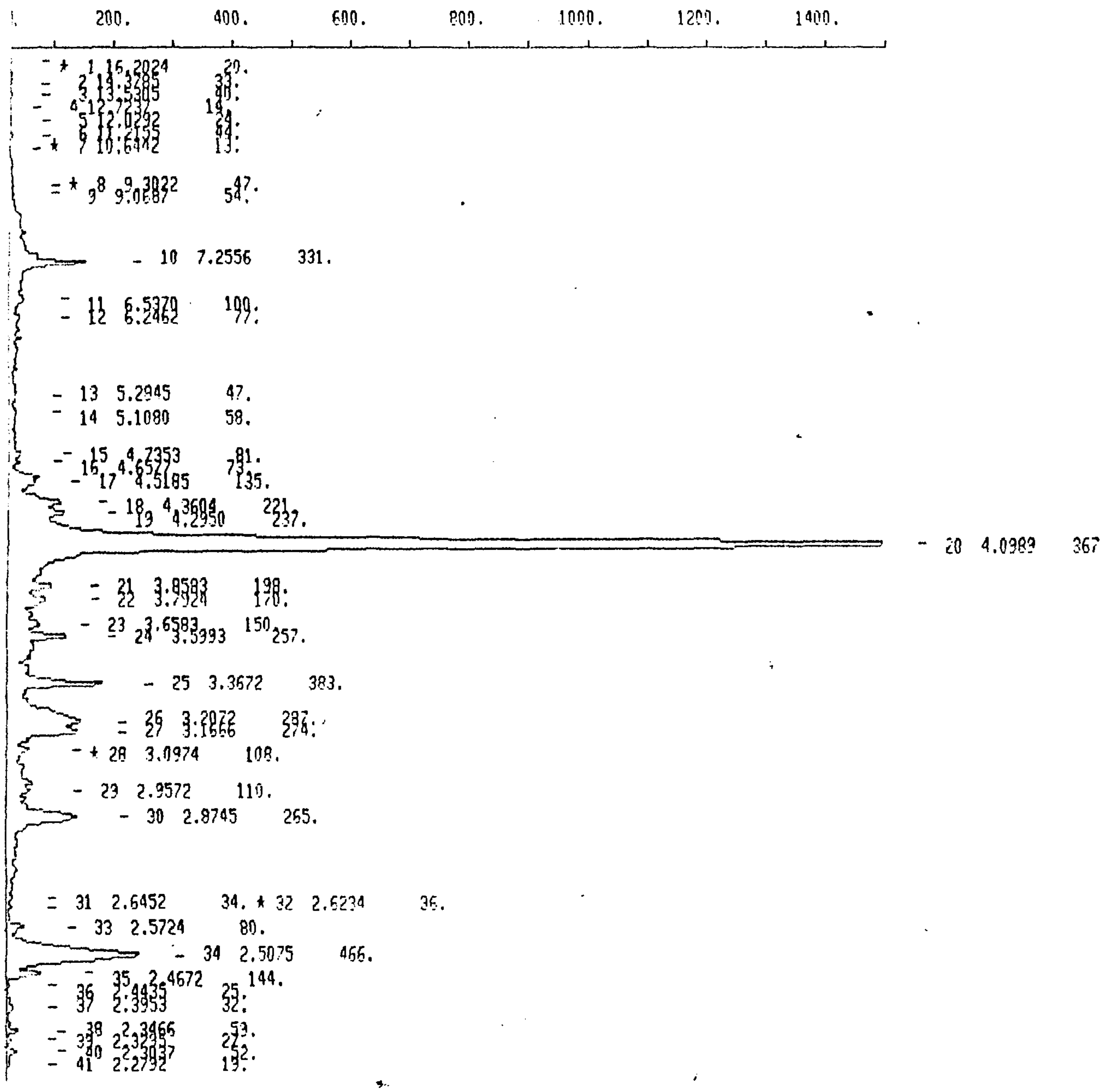

Fig (IV-19) Sample No B8 N

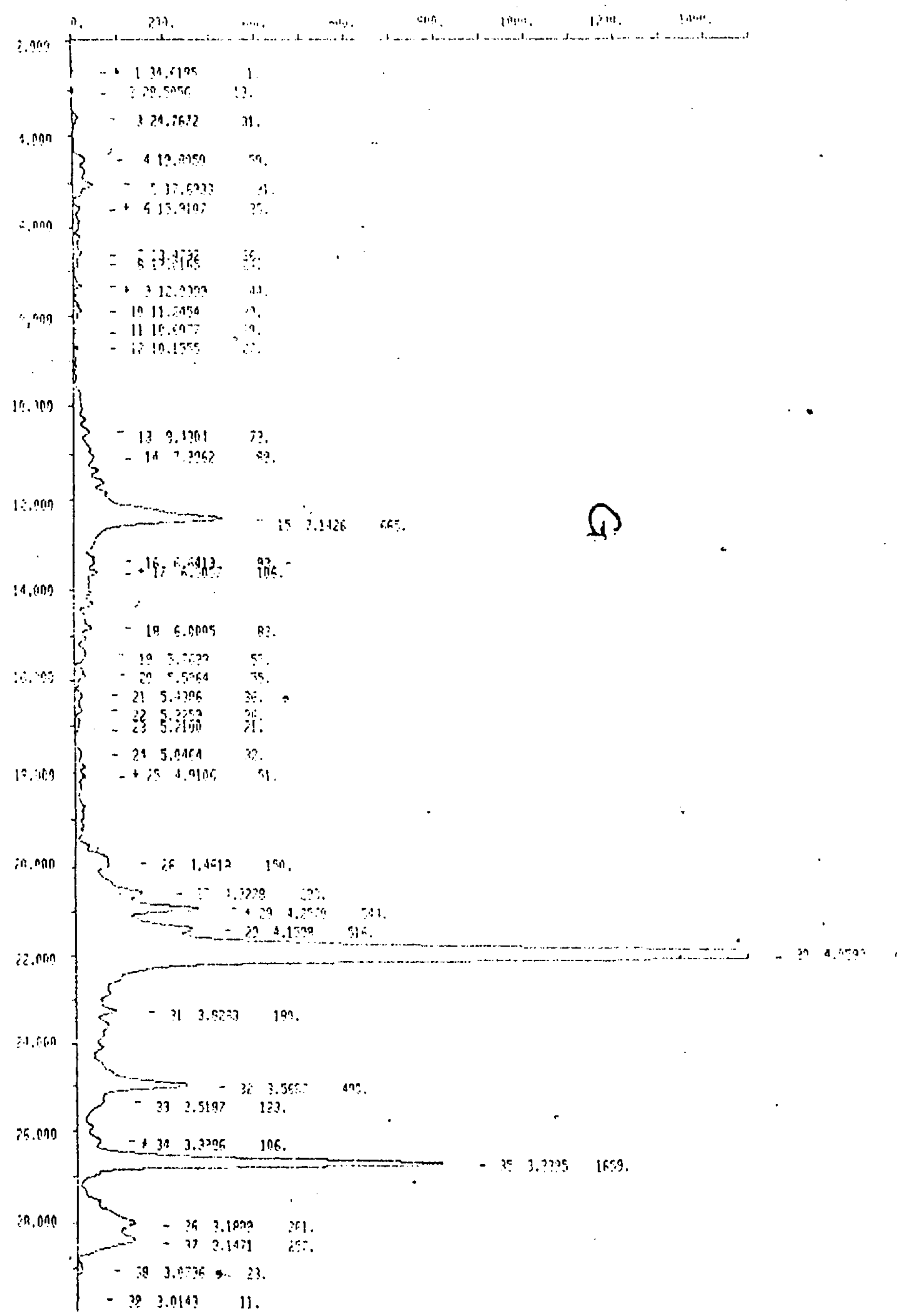

Fig (IV-19) Sample No B8 G

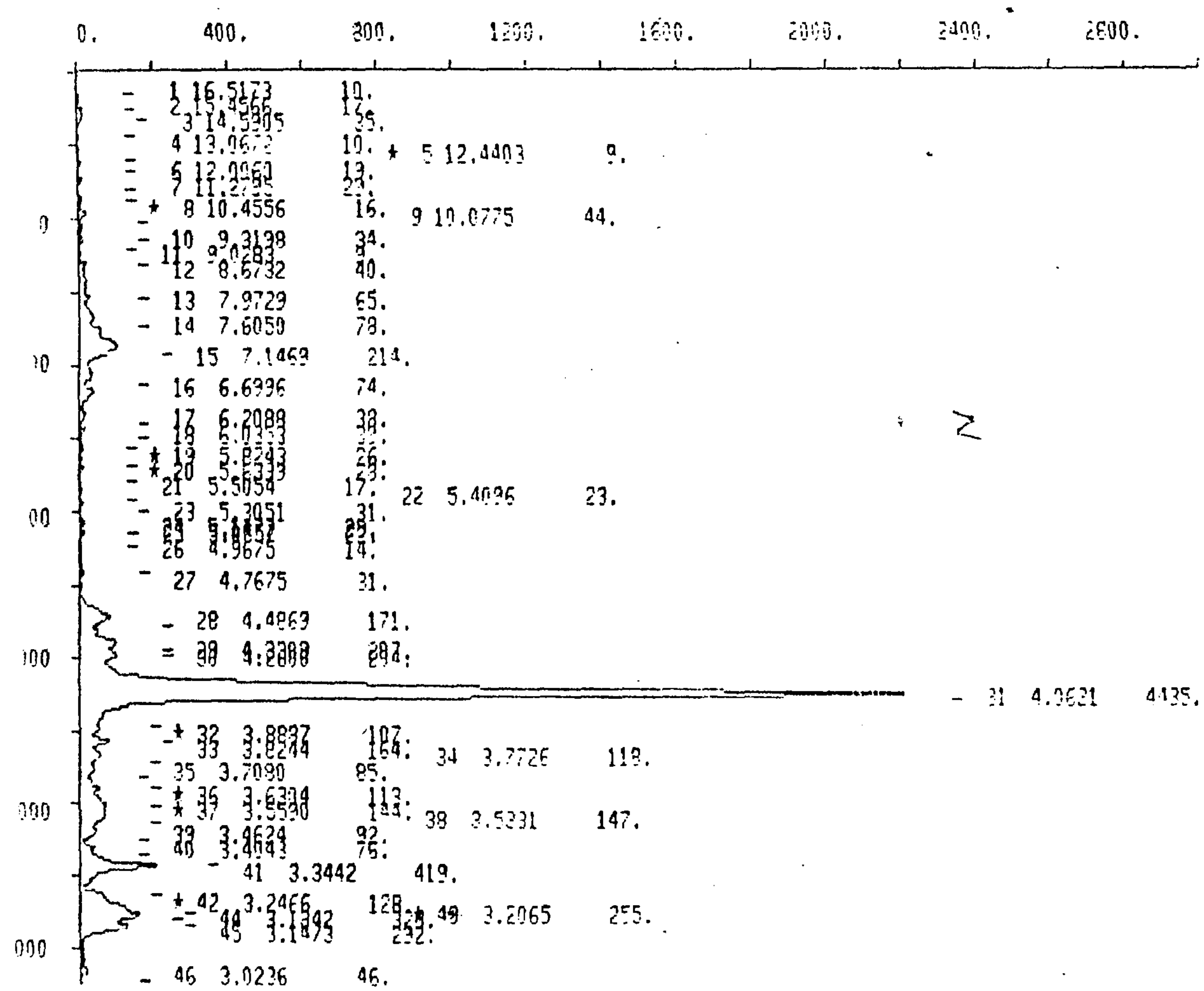

Fig (IV-20) Sample No B10 N

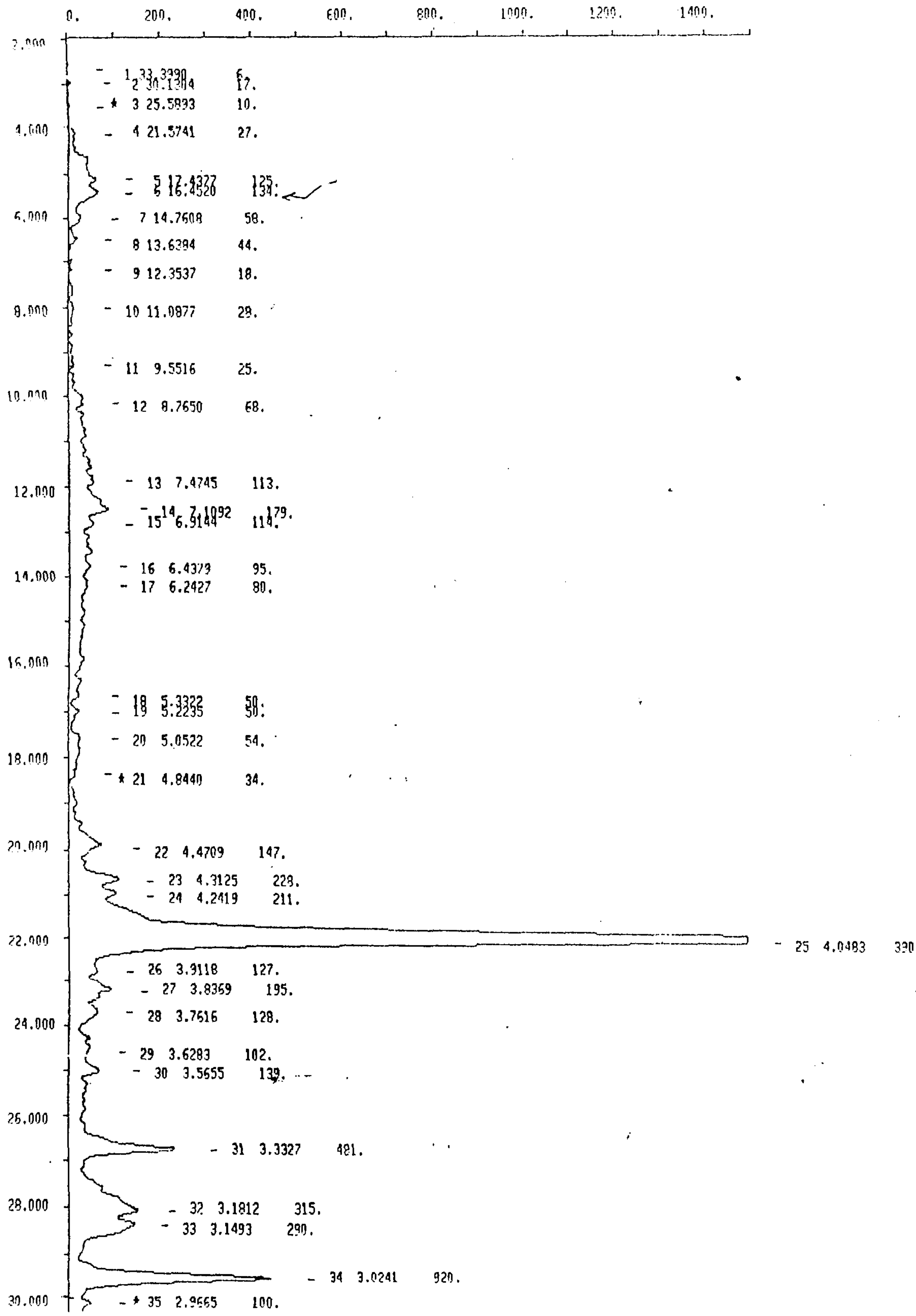

Fig (IV-21) Sample No B10 G

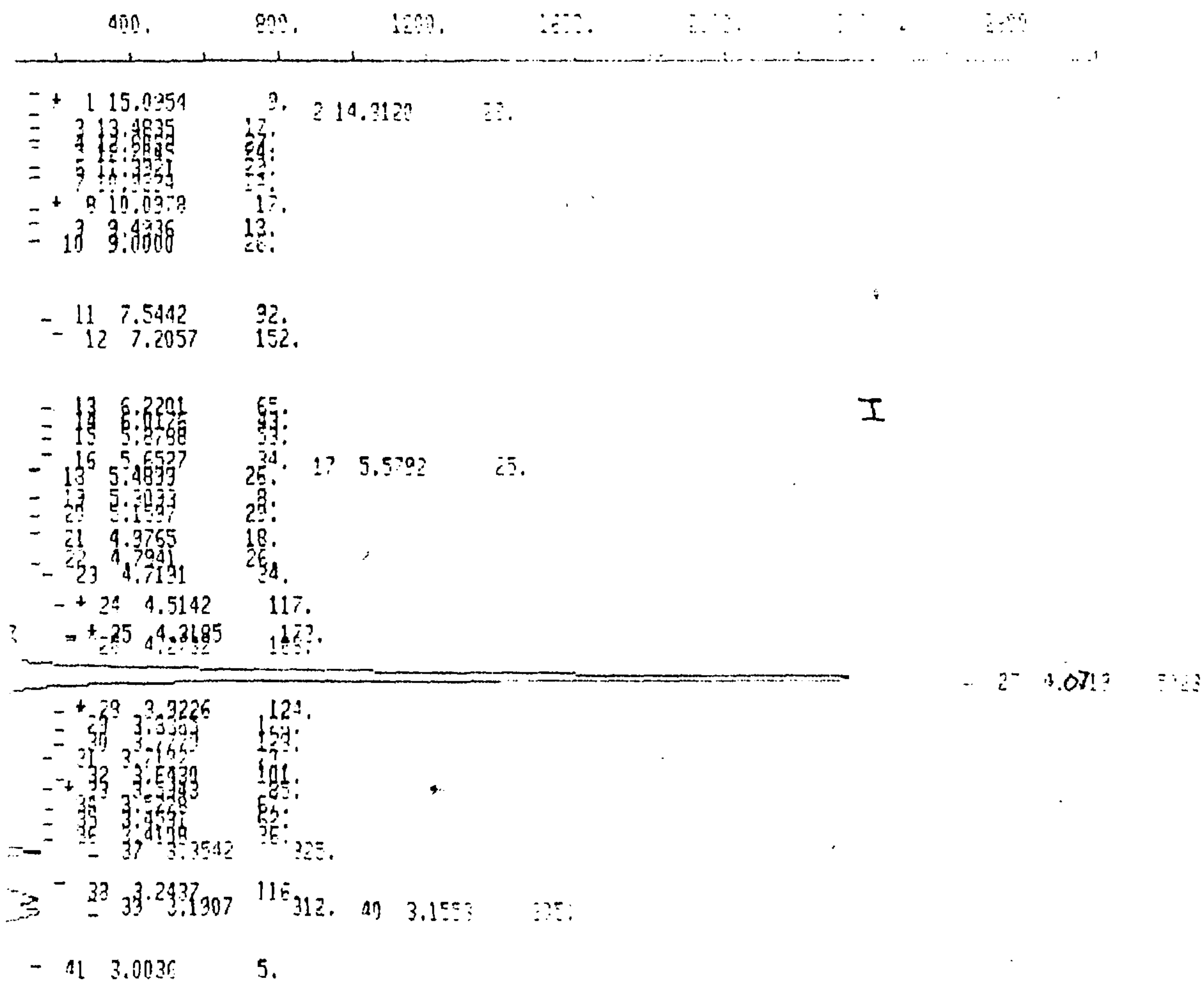

Fig (IV-22) Sample No B10 H

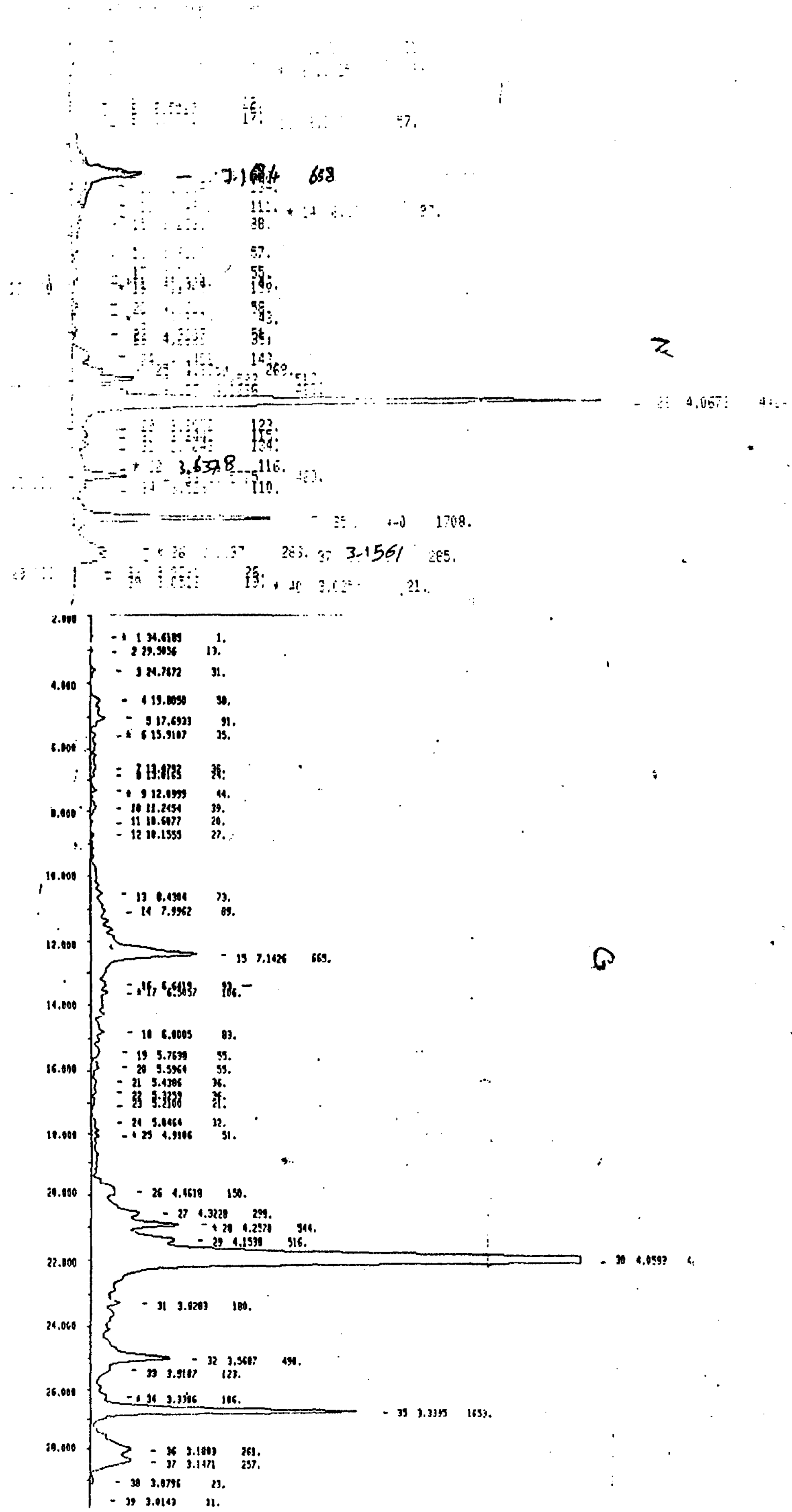

Fig (IV-23) Sample No 8 N,G

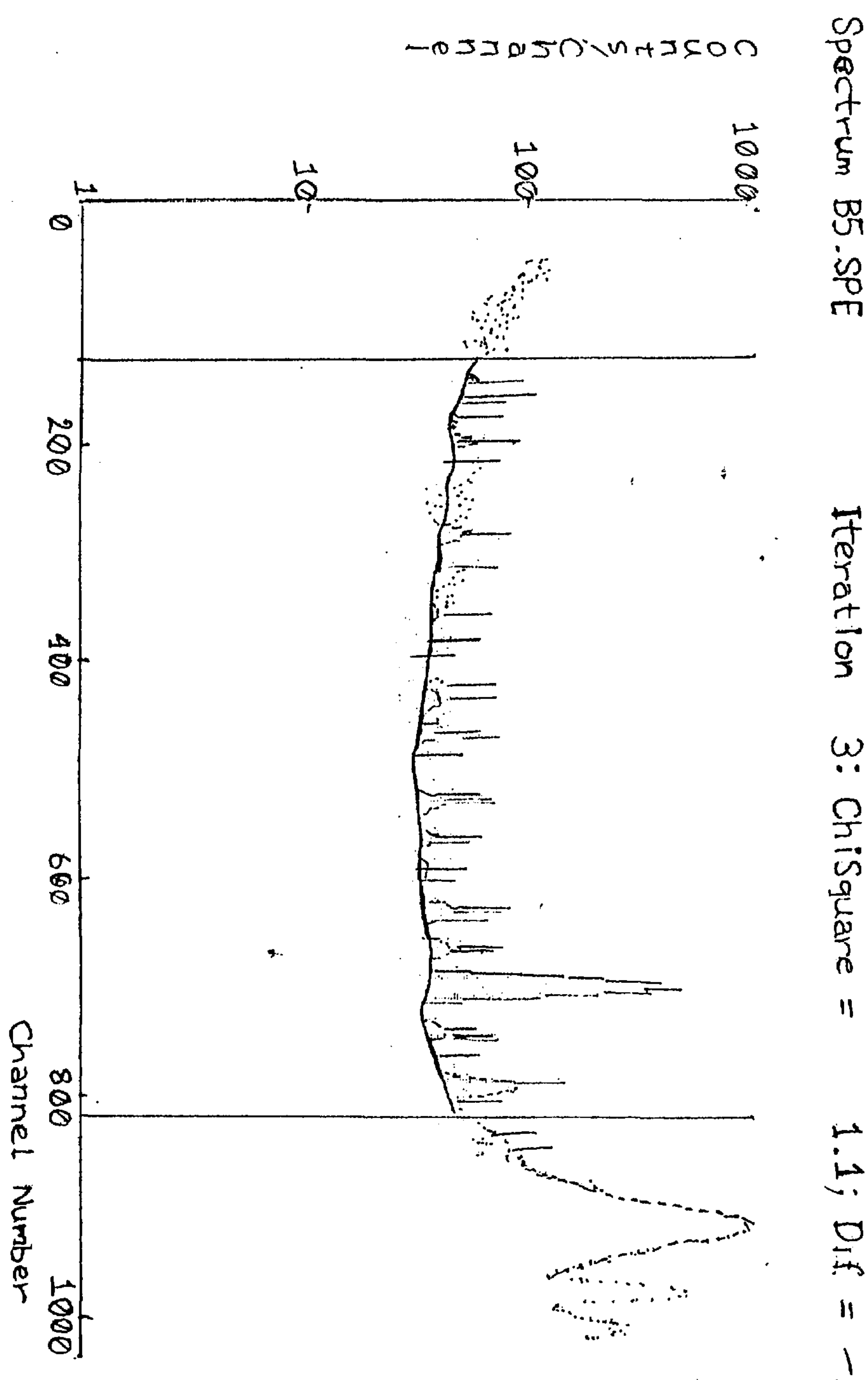

Fig (IV-24) Spectrum of sample B5

FUND4 05-20-1996 12:47:08

Sample identity: NO_ID
Spectrum fitting data: C:\AXIL\SPECT\B5.ASR
Instrument parameter data: a:\AXIL\SPECT\CD109.FPC

Instrumental identity: Isotopic Source
Average instrumental constant: 5.8520E+01
Radio-isotope: Cd-109
Measuring date: 05-18-1996 00:00:00
Reference date: 01-10-1996 14:11:46
Correction factor: .8250
Measuring time: 1000. Sec. Collimator: No Collimator
Filter used: No Filter Atmosphere: Air

Report of Calculated Concentrations.

Sample thickness: 3.0600E-01 g/cm2
Iterations for concentration: 5
Pre-set convergence: .10 % Last convergence: .089 %

Ele.-line	Constituent	Concen.(elem.)		Absorption	Enhancement
Fe-Ka	Fe	3639.75± 671.160	ppm	6.2221E-03	1.0072
Co-Ka	Co	< 1213.68	ppm	7.5505E-03	1.0071
Sr-Ka	Sr	310.09± 48.295	ppm	1.7217E-02	1.0007
Y -Ka	Y	156.95± 36.762	ppm	1.9234E-02	1.0007
Zr-Ka	Zr	4189.54± 77.498	ppm	2.1347E-02	1.0000
Nb-Ka	Nb	100.21± 28.116	ppm	2.2231E-02	1.0000
Mo-Ka	Mo	< 85.40	ppm	2.3680E-02	1.0000

Total percent of fluorescent elements: .95 %
Dark matrix is known as: silol .00

Table (IV-25) Result of sample B5

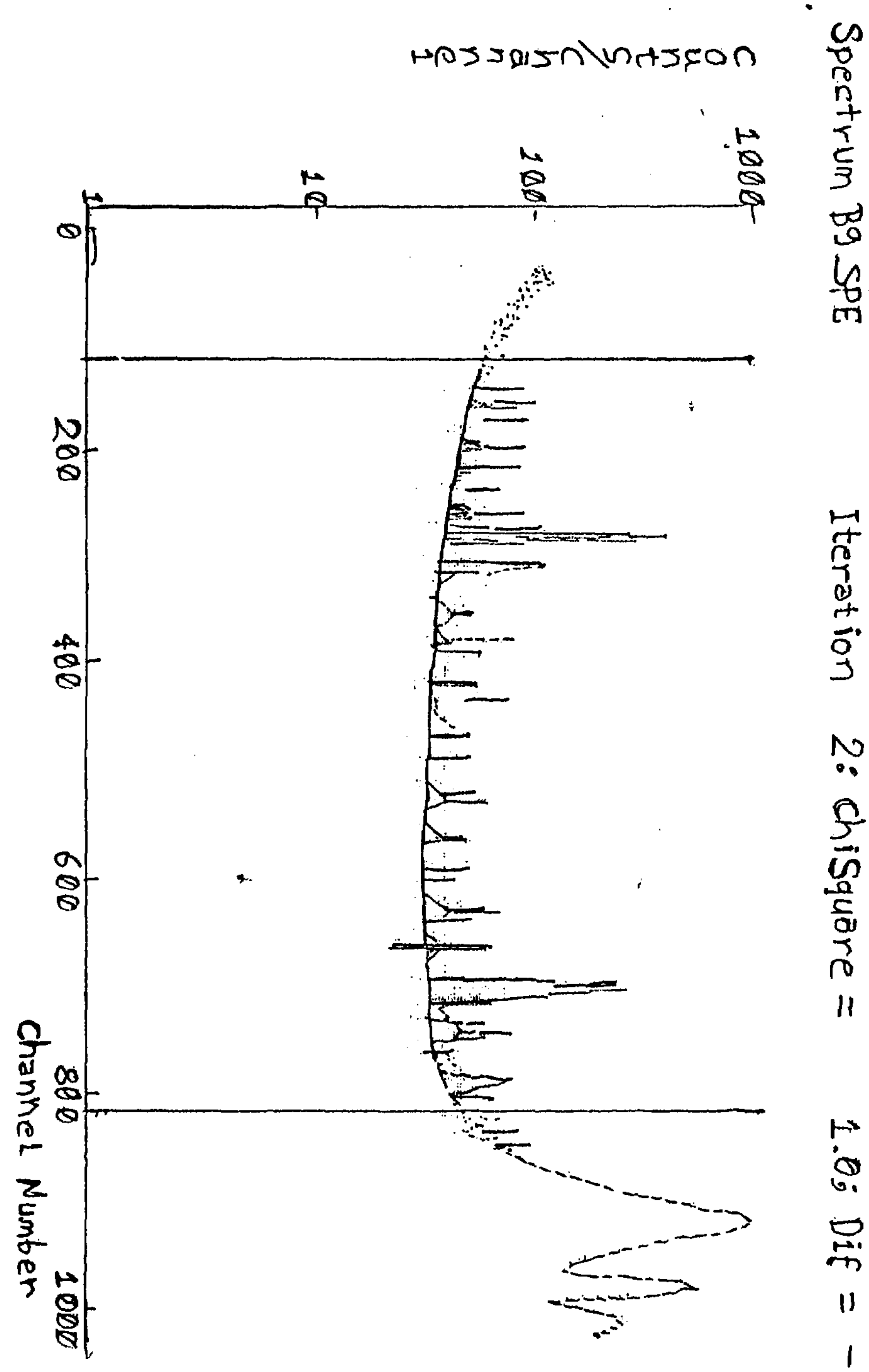

Fig (IV-26) Spectrum of sample B9

FUND4 05-20-1996 13:47:16

Sample identity: NO_ID
Spectrum fitting data: C:\AXIL\SPECT\B9.ASR
Instrument parameter data: a:\AXIL\SPECT\CD109.FPC

Instrumental identity: Isotopic Source
Average instrumental constant: 5.8520E+01
Radio-isotope: Cd-109
Measuring date: 05-18-1996 00:00:00
Reference date: 01-10-1996 14:11:46
Correction factor: .8250
Measuring time: 1000. Sec. Collimator: No Collimator
Filter used: No Filter Atmosphere: Air

Report of Calculated Concentrations

Sample thickness: 3.4690E-01 g/cm2
Iterations for concentration: 4
Pre-set convergence: .10 % Last convergence: .048 %

Ele.-line	Constituent	Concen.(elem.)		Absorption	Enhancement
Fe-Ka	Fe	3.06± .075	%	1.0279E-02	1.0037
Co-Ka	Co	1146.11± 253.647	ppm	1.2514E-02	1.0036
Sr-Ka	Sr	254.80± 51.370	ppm	1.3252E-02	1.0004
Y -Ka	Y	144.79± 39.778	ppm	1.5081E-02	1.0004
Zr-Ka	Zr	2371.81± 66.978	ppm	1.7075E-02	1.0000
Nb-Ka	Nb	141.90± 30.100	ppm	1.8996E-02	1.0000
Mo-Ka	Mo	< 79.03	ppm	2.1122E-02	1.0000

Total percent of fluorescent elements: 3.47 %
Dark matrix is known as: silol .00

Table (IV-27) Result of sample B9

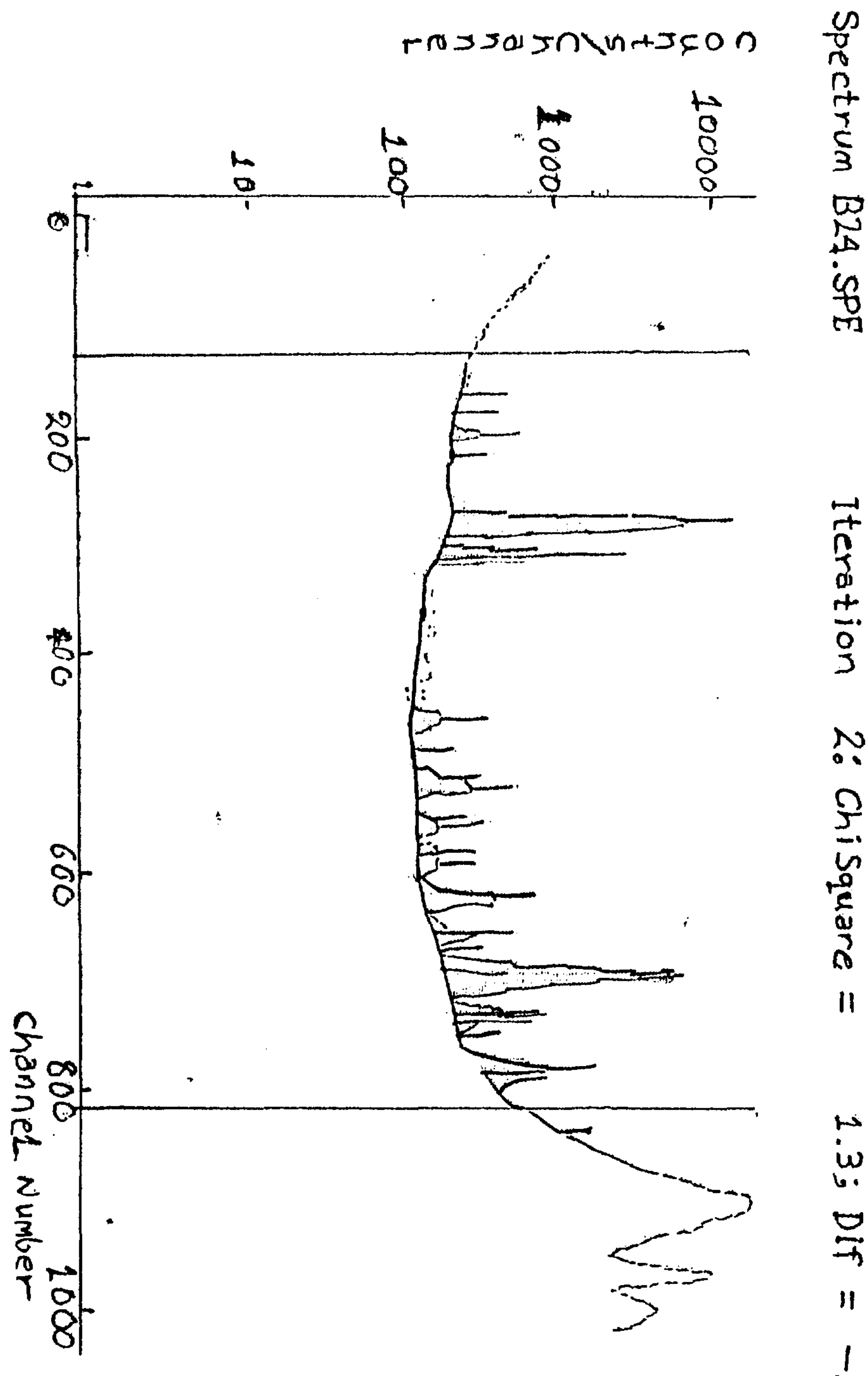

Fig (IV-28) Spectrum of sample B24

B24 05-20-1996 14:09:10

Sample identity: NO_ID
Spectrum fitting data: A:\AXIL\SPECT\B24.ASR
Instrument parameter data: A:\AXIL\SPECT\CD1091.FPC

Instrumental identity: Isotopic Source
Average instrumental constant: 5.8520E+01
Radio-isotope: Cd-109
Measuring date: 05-20-1996 00:00:00
Reference date: 01-09-1996 13:45:03
Correction factor: .8219
Measuring time: 700. Sec. Collimator: No Collimator
Filter used: No Filter Atmosphere: Air

Report of Calculated Concentrations

Sample thickness: 4.0800E-01 g/cm2
Iterations for concentration: 7
Pre-set convergence: .10 % Last convergence: .068 %

Ele.-line	Constituent	Concen.(elem.)			Absorption	Enhancement
Ca-Ka	Ca	4.49±	.681	%	2.2153E-03	4.1458
Ti-Ka	Ti	4.98±	.264	%	3.4607E-03	3.7009
Fe-Ka	Fe	145.99±	.512	%	7.8068E-03	1.1800
As-Ka	As	6101.61±	426.030	ppm	5.5931E-03	1.1699
Se-Ka	Se	< 865.16		ppm	6.5346E-03	1.1506
Br-Ka	Br	1.04±	.033	%	7.5607E-03	1.1463
Kr-Ka	Kr	3206.50±	220.999	ppm	8.7489E-03	1.1343
Rb-Ka	Rb	574.62±	169.194	ppm	1.0058E-02	1.1244
Sr-Ka	Sr	9770.58±	225.037	ppm	1.1410E-02	1.0226
Y -Ka	Y	3618.90±	151.437	ppm	1.2956E-02	1.0151
Zr-Ka	Zr	8.20±	.040	%	1.4673E-02	1.0009
Nb-Ka	Nb	5388.64±	135.401	ppm	1.6377E-02	1.0000

Total percent of fluorescent elements: 167.57 %
Dark matrix is known as: silo1 .00

Table (IV-29) result of samlpe B24

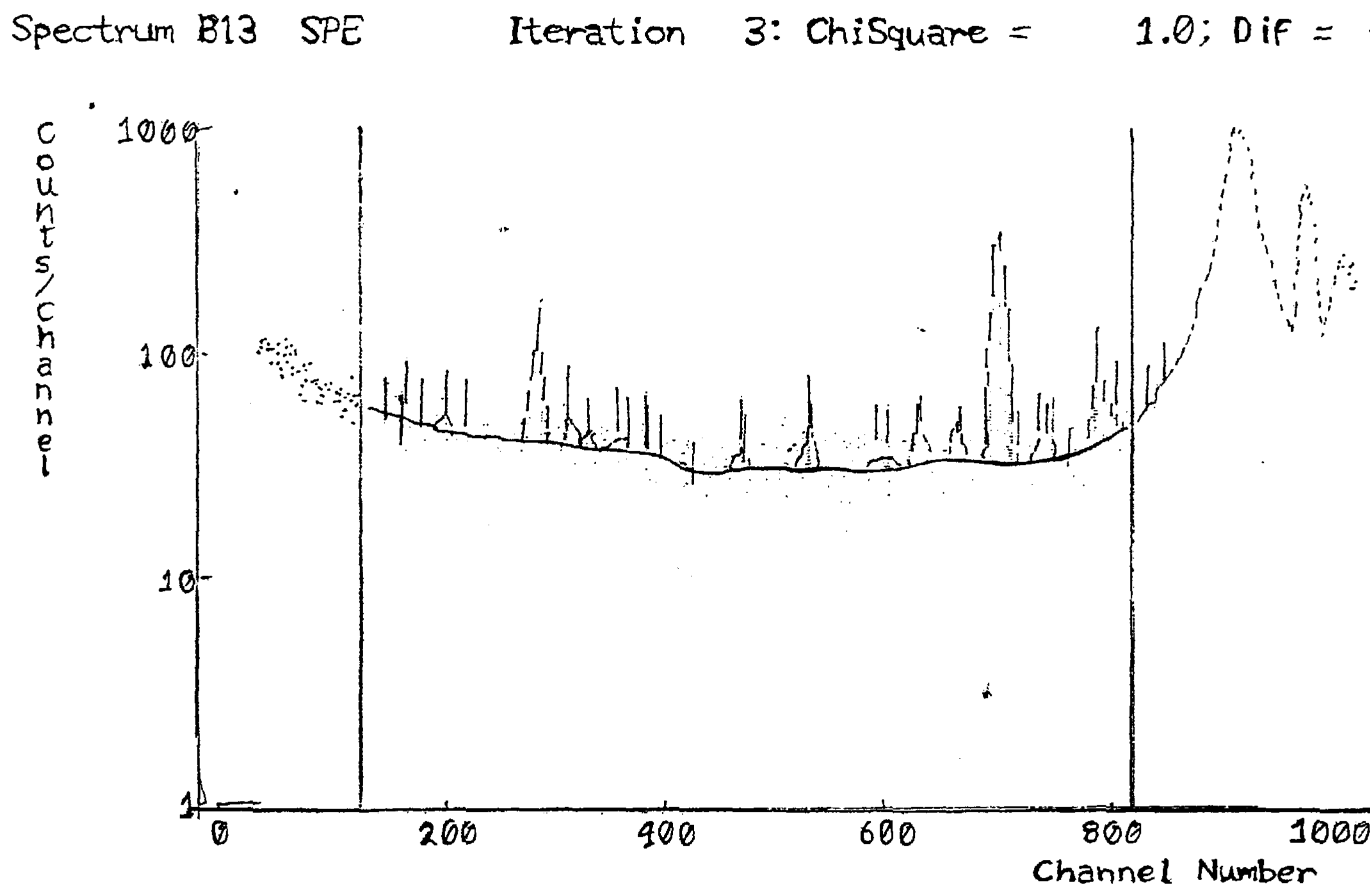

Fig (IV-30) Spectrum of sample B13

```
FUND4                                05-20-1996        13:46:59

Sample Identity: NO_ID
Spectrum fitting data: C:\AXIL\SPECT\B13#.ASR
Instrument parameter data: a:\AXIL\SPECT\CD109.FPC

Instrumental identity: Isotopic Source
Average instrumental constant:  5.8520E+01
Radio-isotope: Cd-109
Measuring date: 05-10-1996 00:00:00
Reference date: 01-10-1996 14:11:46
Correction factor:        .8250
Measuring time: 1000. Sec.     Collimator: No Collimator
Filter used: No Filter          Atmosphere: Air

                 Report of Calculated Concentrations

Sample thickness: 3.0600E-01 g/cm2
Iterations for concentration:    5
Pre-set convergence:   .10 %   Last convergence:   .049 %
```

Ele.-line	Constituent	Concen. (elem.)	Absorption	Enhancement
Fe-Ka	Fe	1.17 ± .066 %	8.7576E-03	1.0055
Sr-Ka	Sr	328.10 ± 52.429 ppm	1.5894E-02	1.0006
Zr-Ka	Zr	3325.84 ± 73.012 ppm	2.0195E-02	1.0000
Nb-Ka	Nb	149.93 ± 29.774 ppm	2.1770E-02	1.0000
Mo-Ka	Mo	< 83.01 ppm	2.4195E-02	1.0000

Total percent of fluorescent elements: 1.55 %

Dark matrix is known as: silol / .00

Table (IV-31) Result of sample B13

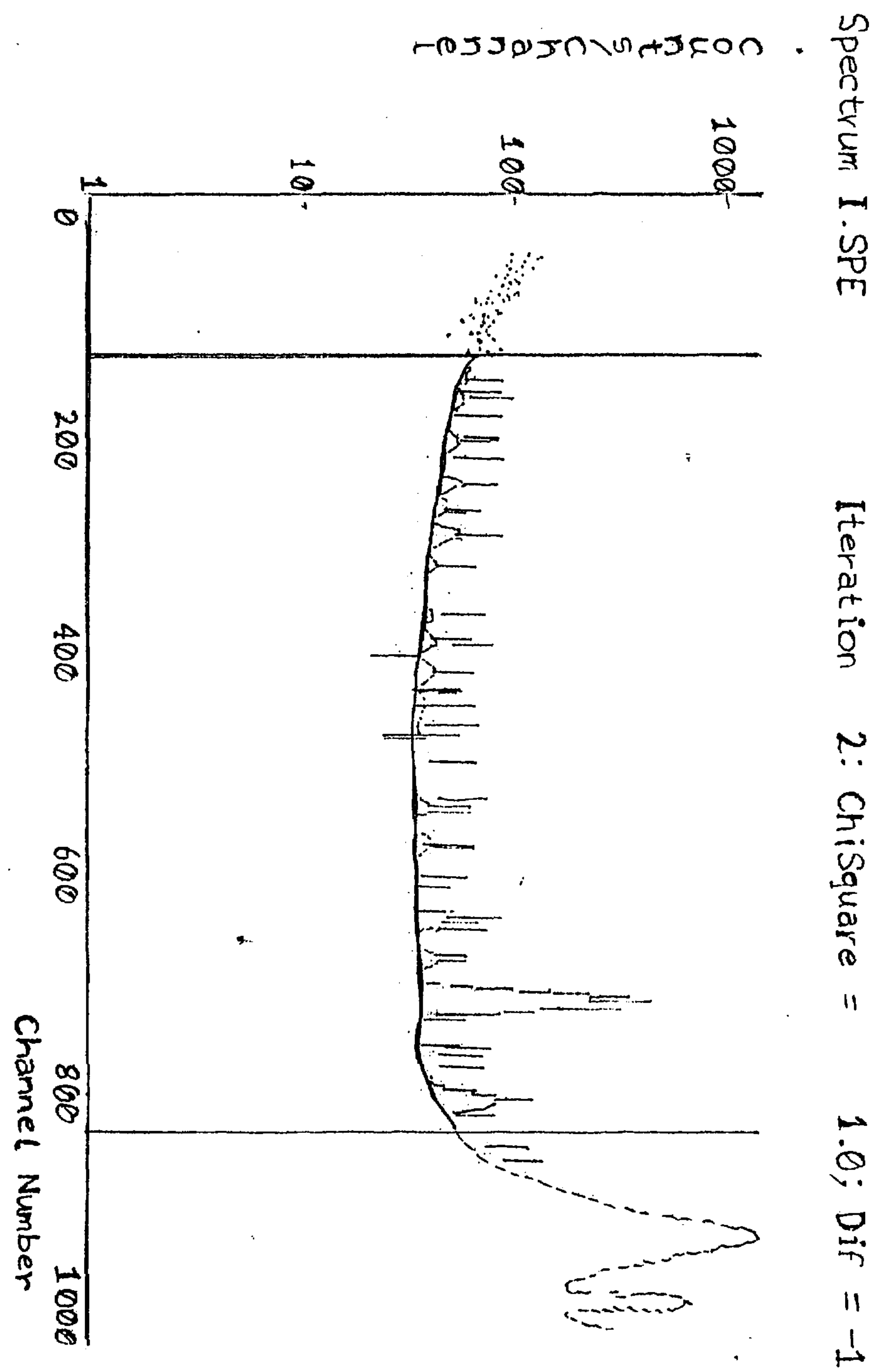

Fig (IV-32) Spectrum of sample I

FUND4 05-20-1996 13:45:57

Sample identity: NO_ID
Spectrum fitting data: C:\AXIL\SPECT\I.ASR
Instrument parameter data: a:\AXIL\SPECT\CD109.FPC

Instrumental identity: Isotopic Source
Average instrumental constant: 5.8520E+01
Radio-isotope: Cd-109
Measuring date: 05-16-1996 00:00:00
Reference date: 01-10-1996 14:11:46
Correction factor: .8274
Measuring time: 1000. Sec. Collimator: No Collimator
Filter used: No Filter Atmosphere: Air

Report of Calculated Concentrations

Sample thickness: 4.8900E-01 g/cm2
Iterations for concentration: 6
Pre-set convergence: .10 % Last convergence: .071 %

Ele.-line	Constituent	Concen.(elem.)	Absorption	Enhancement
Fe-Ka	Fe	5934.10± 682.087 ppm	4.4131E-03	1.0059
Sr-Ka	Sr	367.13± 52.969 ppm	1.0542E-02	1.0006
Y -Ka	Y	109.24± 38.725 ppm	1.1831E-02	1.0006
Zr-Ka	Zr	3548.41± 73.324 ppm	1.3195E-02	1.0000

Total percent of fluorescent elements: 1.00 %
Dark matrix is known as: silol .00

Table (IV-33) Result of sample I

CHAPTER V

SUMMARY AND CONCLUSION

This study has reviewed the theoretical and experimental aspects of the XRD method, and its application in analysing some mudrocks from north western Sudan.

The XRD analysis shows that these mudrocks are composed in decreasing abundances of kaolinite, smectite, chlorite and illite. Other non-clays reported include quartz, feldspar and geothite.

The dominance of kaolinite over other clay minerals indicates that the mudrocks underwent intense chemical weathering and leaching under rather warm humid climatic conditions in north western Sudan during the past geological time. This suggestion ia supported by other geological evidence found in that area. The relative increase of smectite, illite and chlorite may suggest that the humid climate was interupted by dry periods, where direct-physical weathering of the parent rocks was active.

The variation of the chemical elements concentration in the samples studied may be attributed to the difference in clay mineralogy which is controlled by the geology , type and intensity of weathering, local environment, physiochemical behaviour of elements and the prevailing climatic conditions.

It is suggested that further work can be done in determing the site occupancy using X-ray diffraction in combination with X-ray flourescence emission micro analysis.

REFRENCES

1. Alexander O.E Animalu, (1981) "Intermediate Quantum Theory of Crystalloid Solids". Prentice Hall of India private limited, New Delhi.

2. Chamley, I.H.(1989). "Clay sedimentology" printed in Germany.

3. Cullity B.D," Element of X-ray Diffraction" (Addision Weslen publishing company), INC, London (1978).

4. Curtis, C.D and Spears, D.A (1968) "The formation of Sedimentary iron minerals.

5. DACO-MP User's reference V2.1,V2.2 Manual (1985).

6. DACO-MP Getting Started Manual V2.1, V2.2 (1985).

7. DIFFRAC-AT V3.1 Start up Manual (1992), progress in Automation Siemens.

8. DIFFRAC-AT V3.1 EVA User's Guide Manual (1992), progress in Automationiemens.

9. Grim,R.E (1968), "Clay Minerology" pp.596 Mc Grow-Hill, Book, CAMPANY. INC New York.

1 . El Hussein, H. H(1994), "X-Ray Diffraction Studies of Clays & Minerals" M.Sc Thesis, Uof K.

11. Manson, B.(1952) "Principles of Geochemistry".

12. Millot, G. (1970) "Geology of Clays" pp 429. springer-Verlag, New York.

1 . Pieser H. S Book by H.P & Wilson A. J. C, (1955) "X-Ray Diffraction of Polycrystalline Materials". London

14. Nuffield E.W (1966) "X-ray Diffraction Methods" John Wiley and sons, INC, New York.

1 . Siemens D500/ D501 Diffractometer Operating Instruction Manual. Model No 79000-B3400-Co42-10.

16. Thorez. J (1976). "Practical Identification of Clay Minerals ".G. LELOTTE B.4820 DISON. Belgique.

17. Tucker M. (1991). "Sedimentary Petrology and Introduction to the origin of sedimentary Rocks" Black Well Scientific public publications", Oxford OX2 OEL 8 John Street.

18. Tucker M. (1988). "Techniques in Sedimentology Black Well Scientific public publications", Oxford OX2 OEL 8 John Street.

19. Weaver, C. E (1989) "Clays, Muds and Shales Development in Sedemintology" 44, p 819.